筑　波　大　学

博 士 （ 医 学 ） 学 位 論 文

Stratifin regulates stabilization of receptor tyrosine kinases via activation of ubiquitin-specific protease 8 in lung adenocarcinoma

(Stratifin は ubiquitin-specific protease 8 を 活性化することにより受容体型 チロシンキナーゼの分解を抑制する)

2017

筑波大学大学院博士課程人間総合科学研究科

Kim YunJung

TABLE OF CONTENTS

List of figures

List of table

Abstract

[Purpose]

Receptor tyrosine kinases (RTKs) such as epidermal growth factor receptor (EGFR) and hepatocyte growth factor receptor (MET) are the best-known targets of therapy for non-small cell lung cancer (NSCLC). Previously, our laboratory has revealed that stratifin (SFN, 14-3-3 sigma) acts as a novel oncogene, accelerating tumor initiation and progression of lung adenocarcinoma and interacts with ubiquitin-specific protease 8 (USP8). In this study, I investigated whether stratifin (14-3-3 σ or SFN) enhances RTK stabilization through abnormal USP8 activation in lung adenocarcinoma.

[Materials and Methods]

Expressions of USP8 and SFN in human lung adenocarcinoma tissues (n=193) were examined by immunohistochemistry and statistically analyzed with clinicopathological features of patients. Functional analysis of USP8 and SFN such as cellular proliferation assay, apoptosis assay, and wound healing assay was examined after siRNA-USP8 or SFN transfection. Regulation mechanism of USP8 and SFN on RTKs stabilization was demonstrated using co-immunoprecipitation, western blot analysis, and immunofluorescence analysis.

[Results]

USP8 specifically bound to SFN in lung adenocarcinoma cells. Both USP8 and SFN showed higher expression in human lung adenocarcinoma than in normal lung tissue, and USP8

expression was significantly correlated with SFN expression. Expression of SFN, but not that of USP8, was associated with histological subtype, pathological stage, and prognosis. *In vitro*, USP8 binds SFN at the early- and late-endosome in immortalized adenocarcinoma *in situ* (AIS) cells. Moreover, USP8 or SFN knockdown led to down-regulation of tumor cell proliferation, RTK expression, and expression of downstream factors including AKT and STAT3, as well as accumulation of ubiquitinated RTKs for lysosomal degradation. Additionally, transfection with mutant USP8 and mutant SFN, which are unable to interact each other, reduced the expression of RTKs and their downstream factors.

[Discussion]

RTKs are regulated by ubiquitin-lysosome system, and aberrant stabilization of RTKs contributes to the proliferative activity of many human cancers, including NSCLC. Base on the IHC results, the biological effect of USP8 might be included in that of the multi-function proteins, SFN and the expression of USP8 itself may not influence the final outcome. From the facts that phospho-USP8 binds to SFN and knockdown of SFN reduces the levels of USP8 protein, abnormal overexpression of SFN in lung adenocarcinoma might promote interaction with USP8 and induce a conformational change of USP8 that may result in an acceleration of its enzymatic activity and stability. Therefore, a SFN inhibitor would be a more selective and desirable therapeutic target for lung adenocarcinoma than USP8.

[Conclusion]

In this study, I demonstrate SFN induces aberrant activation of USP8 and subsequently protects RTKs from lysosomal degradation, resulting in hyperactivation of these signaling

pathways. SFN may be central to the development of a useful therapeutic strategy for both early and advanced lung adenocarcinomas.

1. Introduction

1-1 Current treatment of lung adenocarcinoma

The rate of mortality due to lung cancer increased rapidly in the 20th century for both men and women worldwide (1). The most common histological type of lung cancer is adenocarcinoma, categorized as non-small cell lung cancer (NSCLC), which has a 5-year survival rate of approximately 40%. However, Noguchi *et al.* have demonstrated that adenocarcinoma *in situ* (AIS, type A and B in the Noguchi classification) has an extremely favorable outcome, with a 5-year survival rate of 100% (2). AIS shows stepwise progression to early but invasive adenocarcinoma (eIA, type C in the Noguchi classification), which has a relatively poorer outcome (Fig.1) (3).

According to extensive molecular analyses, lung adenocarcinoma cells is well-known to harbor various genetic alterations which induce many events including up-regulation of oncogenes, down-regulation of tumor suppressor genes, and resistance to apoptotic cell death, thus facilitating tumor progression. The frequencies of some genetic alterations significantly differ among populations. In the case of Japan patient's population, mutation of receptor tyrosine kinases (RTKs) including epidermal growth factor receptor (EGFR), human epidermal receptor 2 (HER2), and hepatocyte growth factor receptor (MET) are the most common driver mutation (Fig.2) (4).

Within recent several years, diverse new-targeted therapies including EGFR-targeting drug such as gefitinib and erlotinib, anaplastic lymphoma kinase (ALK)/proto-oncogene1 (ROS1)-targeting drug such crizotinib have approved for advanced stage of lung adenocarcinoma. Despite these treatments provide remarkable effect for patients who are

harboring specific genetic alteration, the most drugs lead acquired drug resistance, induction of second mutation, and high toxicity against wild-type form.

Unlike the current treatment strategy for advanced adenocarcinomas, no therapeutic approach for early-stage lung adenocarcinomas such as adenocarcinoma *in situ* (AIS) has yet been established, except surgical resection. Moreover, the number of genetic alteration such as EGFR, K-RAS, and p16 inactivation is limited in early-stage lung adenocarcinoma (Fig.1). Thus, discovering biomarker for early-stage of lung carcinoma is essential for early diagnosis and targeting therapy.

1-2 The characteristic of stratifin (SFN) in lung adenocarcinoma

Stratifin (SFN, 14-3-3 sigma) is the most distinct member of the highly conserved 14-3-3 protein family (5), which includes the beta, epsilon, eta, gamma, tau, zeta, and sigma isoforms (Fig. 3A) (6). All 14-3-3 proteins can form both homo- and hetero-dimers, except that SFN prefers homo-dimers, and bind to a specific phospho-serine/threonine-containing motif on various proteins (Fig. 3B) (7). 14-3-3 proteins are ubiquitously expressed in human tissue. Although each of the 14-3-3 isoforms has unique tissue-specific functions, SFN is the form most directly related to tumor initiation and progression in the early lung adenocarcinoma (7, 8). Physiological SFN acts as an adaptor protein that controls signal transduction, protein trafficking, the cell cycle, and apoptosis (9). However, modification of SFN expression occurs in many human cancers including lung, skin, breast, endometrium, head and neck, liver, and prostates. Aberrant expression of SFN in various cancers is caused by different CpG methylation status.

For example, unlike hypermethylation of SFN in breast cancer (10), hypomethylation in SFN promoter participates in the overexpression of SFN to accelerate lung tumor progression (11). Nevertheless, lung tissue specific molecular network of SFN to contribute tumor progression has been unknown.

Previously, our group attempted to screen factors that bound specifically to SFN. In order to identify SFN binding partners in lung adenocarcinoma cells, A549 cells were transfected with SFN vectors and subjected to pull-down assay and LC-MS/MS analysis. Among the candidate proteins, I focused on USP8 as a direct binding partner of SFN in this study.

1-3 The characteristic of ubiquitin-specific protease 8 (USP8) in lung adenocarcinoma

USP8 is a ubiquitin-specific protease (USP), being one of the deubiquitinating enzymes (DUBs) that stabilize specific protein substrates by removing ubiquitin from them (12). USP8 contains microtubule interacting and transport domain (MIT domain, residues 8-137), rhodanese-like domain (Rho domain, residue 185-310), two Src homology 3(SH3)-binding domains (SH3 domains, residues 405-413 and 700-708), 14-3-3 binding motif (residues 715-720), and deubiquitinase catalytic domain (DUB domain, residues 774-1106) with the conserved boxes surrounding the catalytic cysteine (residues 778-793) and histidine (residues 1051-1068) (Fig. 4) (13).

USP8 has already been reported to target several particular substrates, including G-protein-coupled receptors (smoothened and frizzed) (14, 15), neuregulin receptor degradation protein-1 (Nrdp1) (16), and RTKs (17-19), which are involved in a number of human diseases

including malignant neoplasms. However, the mechanisms responsible for controlling the deubiquitination activity of USP8 and mutation or expression level of USP8 in lung adenocarcinoma are still poorly understood. Among the various targets of USP8, RTKs such as EGFR and MET are the best-known therapeutic targets in lung cancer (20). Moreover, USP8 has been reported to be a novel therapeutic target for tyrosine kinase inhibitor (TKI)-resistant and -sensitive NSCLS, as USP8 inhibition induces degradation of RTKs (21). Even though inhibition of USP8 is beneficial for overcoming TKI resistance, it can be easily envisaged that this might have various side effects in view of its influence on the normal physiological function of USP8. Supportively, USP8 was first demonstrated as a growth-regulated ubiquitin isopeptidase (22), deletion of which caused embryonic lethality in mice (23), implying that the normal physiological function of USP8 is crucial for cell survival.

1-4 The regulation mechanism of receptor tyrosine kinases (RTKs) in lung adenocarcinoma

1-4-1 The role of RTKs in lung adenocarcinoma

In normal cells, ligand-mediated RTKs activation such as EGFR and MET is strictly controlled (Fig. 5). Activated RTKs undergo rapid endocytosis and subsequent degradation in lysosomes within a couple of hours (24). This process contributes to down-regulation of downstream signaling by which activation of RTKs is cancelled, resulting in abolition of over-proliferation (25). Meanwhile, activated RTKs lead to multiple downstream signaling events such as AKT, ERK, and STAT3 pathways that control various processes including cellular proliferation, cell survival, differentiation, invasion, angiogenesis, and cell migration (26).

Overexpression of RTKs typically correlates with poor prognosis reflected in the unfavorable progression free survival and overall survival. Active somatic mutations of RTKs are found particularly in NSCLC patients. The most prominent mutations in EGFR are found in exon 18-21 in tyrosine kinase domain in which patients harboring the mutations have sensitivity for TKIs treatment such as gifitinib and erlotinib as first generation, afitinib as second generation, and osimetinib as third generation (27). In addition to EGFR mutation, MET gene alterations such as exon 14 internal deletions, point mutations, and gene amplification are oncogenic in NSCLC (28). Favorable responses of anti-MET TKIs such as cabozantinib in MET-mutated NSCLC have been reported. Although these treatments initially have a fast antitumor effect, these patients acquire drug resistance against TKI after a median of 10-16 months for drug administration (26, 29). This phenomenon is thought to be a result of crosstalk among RTKs to escape from therapy. Thus, novel biomarker that can control various RTKs simultaneously is desired to improve patient survival.

1-4-2 Ubiquitination and deubiquitination system of RTKs

Ubiquitination is a post-translational modification mediated by the ubiquitin conjugating system which is composed of E1, E2, and E3 enzymes (30). Ubiquitin addition may take the form of single molecule attachment to one or multiple lysines (mono-ubiquitination) or multiple chain attachment (poly-ubiquitination) with each subsequent ubiquitin attached to a lysine of the prior. Several lysine residues in ubiquitin protein are utilized for chain formation including Lysine 6, (K6), K11, K29, K48, and K63 (31).

Ubiquitination is a reversible modification, as conjugated ubiquitin molecules can be cleaved from target proteins by DUBs. This process is referred to as deubiquitination, recycling

target proteins to enhance their stabilization. These reactions have an important role to determine fate of target proteins.

For example, Cbl is a E3 ubiquitin ligase responsible for K63-linkage medicated ubiquitination of activated RTKs and interacts with phosphotyrosine 1045 and 1003 of EGFR and MET, respectively (32). The activated RTKs with polyubiquitin undergo endocytosis and are sorted into either lysosomal degradation or recycling back to the plasma membrane by endosomal DUBs such as USP8 (33). USP8 functions at two stages of plasma membrane receptor trafficking; at early endosomes or late endosomes.

In this study, I focus on SFN and USP8 function at early endosomes, which cleaves poly-ubiquitin of RTKs to recycle them back to plasma membrane for abnormal distribution of RTKs with downstream signal transduction.

2. Materials and methods

2-1 Patients and sample selection

The specimens of lung adenocarcinomas (n=193) were selected that had been surgically resected at the University of Tsukuba Hospital (Ibaraki, Japan) between 1999 and 2007. Follow-up information for all of the corresponding patients was obtainable from the medical records. Informed consent for use of their materials had been obtained from all of the patients. The study was approved by the Institutional Ethics Review Committee and the lung adenocarcinoma cases were classified according to the UICC TNM classification of malignant tumors (seventh edition) and the World Health Organization (WHO) classification of malignant tumors (fourth edition) (34, 35)

2-2 Immunohistochemistry (IHC)

Four-μm-thick tissue sections were used from formalin-fixed paraffin-embedded (FFPE) tissue microarray (TMA) blocks. Each TMA block comprised 24 specimens containing lung adenocarcinoma tissue in a 48-core slide. The sections were deparaffinized and rehydrated, followed by blocking of endogenous peroxidase using 3% H_2O_2 for 30 min at room temperature. Subsequently, antigen retrieval was performed using an autoclave with 10 mM Tris-EDTA buffer (pH 9.0) at 105°C for 10 min. Immunostaining was performed using a Dako Autostainer Link 48 (Agilent Technologies, Santa Clara, CA) with the appropriate primary antibodies and REAL envision HRP rabbit/mouse (Agilent Technologies) as a secondary antibody. The immunoreactivity was detected with DAB (Dako REAL Envision Detection System; Agilent Technologies), and counterstaining was performed with hematoxylin for 1 min. The evaluation

of USP8 and SFN was according to the intensity of cytoplasmic staining. The staining was judged to be positive when the cytoplasm of the tumor cells was stained more strongly than that of the alveolar epithelium. Testis tissue was used as a positive control for USP8 and lung adenocarcinoma tissue with high SFN expression, which was used for a previous study (36), was used for SFN. Rabbit polyclonal USP8 antibody (Bethyl Laboratories, Montgomery, TX) and mouse monoclonal SFN antibody (Sigma-Aldrich) were used as the primary antibodies.

2-3 Pyro-sequencing analysis

Using a Qiagen QIAamp DNA mini kit (QIAGEN), genomic DNA was extracted from the PL16T, A549, PC9, HCC827, H1650, and H1975 cultured cell lines, and from 10 sets of fresh normal and tumorous human lung tissues resected surgically. Primers used for PCR and pyro-sequencing were designed using QIAGEN software, PyroMark Assay Design 2.0. The sequencing process, and allele quantification (AQ) / genotyping (SNP) assay, were performed using PyroMark24Q with suitable reagents from QIAGEN.

Pyro-sequencing primers

USP8-Sequence primer	GCGGGATAGGGAACC
USP8-Forward (AQ)	ATTATCATTCACCCACCAACACT
USP8-Reverse (AQ)	TCCTCTTGAATAGCCTGGGTTATA-Biotin

2-4 Cell lines and culture conditions

The PL16T cell line was established in our laboratory from a surgically resected AIS of

the lung (37). PL16T was maintained in MCDB153HAA (Wako, Osaka, Japan) supplemented with 2% FBS (Sigma-Aldrich, St. Louis, MO), 0.5 ng/ml human EGF (Toyobo, Tokyo, Japan), 5 μg/ml human insulin (Wako), 72 ng/ml hydrocortisone (Wako), 40 μg/ml human transferrin (Sigma-Aldrich), and 20 ng/ml sodium selenate (Sigma-Aldrich). PC9 and A549 were purchased from RIKEN Cell Bank (Ibaraki, Japan) and H1650, H1975, HCC827 were purchased from the American Type Culture Collection (ATCC, Manassas, VA). The cells maintained in Dulbecco's modified Eagle medium (DMEM) / F12 for A549, in RPMI 1640 for PC9, H1650, and HCC827, and in RPMI 1640 ATCC Modification (Thermo Fisher Scientific, Waltham, MA) for H1975. All mediums were supplemented with 10% FBS. The cells were cultured in a 5% CO_2 incubator at 37°C and passaged every 3-4 days.

2-5 Transfection of small interfering RNA (siRNA)

USP8-specific or SFN-specific siRNAs from Thermo Fisher Scientific and a nucleic acid transfer agent, lipofectamine RNAiMAX (Thermo Fisher Scientific), were incubated together in OPTI-MEM reduced-serum medium (Thermo Fisher Scientific) for 15 min at room temperature to form a siRNA-lipofectamine complex. The medium containing the siRNA-lipofectamine complex was added to the cells to give a final siRNA concentration of 10 nM for A549 and 5 nM for PL16T, PC9, and H1975. The cells were incubated at 37°C in a 5% CO_2 incubator for 24 or 48 h and then further analyzed.

siRNA sequences

siUSP8 #1-Forward	GGACAACCAGAAAGUGGAAUUCUAA
siUSP8 #1-Reverse	UUAGAAUUCCACUUUCUGGUUGUCC
siUSP8 #2-Forward	ACCGAAACUGUUAUCAGGAUGAUAU

siUSP8 #2-Reverse	AUAUCAUCCUGAUAACAGUUUCGGU
siUSP8 #3-Forward	GCAGGAUUAUCAGGAUUCCUGUAUU
siUSP8 #3-Reverse	AAUACAGGAAUCCUGAUAAUCCUGC
siSFN #1-Forward	UCUCAGUAGCCUAUAAGAACGUGGU
siSFN #1-Reverse	ACCACGUUCUUAUAGGCUACUGAGA
siSFN #2-Forward	CCGUCUUCCACUACGAGAUCGCCAA
siSFN #2-Reverse	UUGGCGAUCUCGUAGUGGAAGACGG
siSFN #3-Forward	UGGAGAGAGCCAGUCUGAUCCAGAA
siSFN #3-Reverse	UUCUGGAUCAGACUGGCUCUCUCCA

2-6 Transfection of expression vectors

Expression vectors for full-length wild-type human USP8 was purchased from Addgene (Cambridge, MA). HA-ubiquitin was obtained from Prof. Yasunori Kanaho (University of Tsukuba, Japan). Plasmid DNA was purified using an EndoFree Plasmid Maxi kit (QIAGEN, Hilden, Germany). The day before transfection, PL16T cells were trypsinized, counted, and plated at 8 x 10^4 cells per well in 2 ml of complete growth medium onto 6-well plates to obtain 50% to 80% confluence on the day of transfection. For each well of cells to be transfected, 2.8 μg of plasmid DNA was diluted in 500 μl of OPTI-MEM reduced-serum medium, and then 8.3 μl of Fugene HD (Promega, Madison, WI) was added, followed by incubation for 5 min at room temperature. I performed gentle mixing by rocking the plate back and forth. The cells were incubated at 37°C in a 5% CO_2 incubator for 24 h, after which they were further analyzed.

2-7 DNA plasmid constructs and point mutagenesis

Expression vectors for full-length wild-type human USP8 and both 14-3-3 epsilon and zeta were purchased from Addgene (Cambridge, MA). Construction of Flag-SFN and pSFN has been described previously (36). GFP-USP8 wild type, and GFP-USP8 C786S (DUB inactive) were obtained from Prof. Yasunori Kanaho (University of Tsukuba, Japan). Mutagenesis to create constructs encoding the S718C mutant form of USP8 was carried out with the PrimeSTAR Mutagenesis Basal kit (Takara, Shiga, Japan) in accordance with the manufacturer's protocol. Mutagenesis of SFN was carried out by site-direct mutagenesis PCR. The primer information was list up below. Sequences of all constructs were verified by Sanger sequencing.

Primer for USP8 mutagenesis

USP8 S718A-Forward	TCCTACTGCTCCCCAGATATAACCCA
USP8 S718A-Reverse	TGGGGAGCAGTAGGAGCGCTTCAGTT

Primer for SFN mutagenesis

SFN K49A-Forward	GCCTATGCAAACGTGGTGGGCGGC
SFN K49A-Reverse	CACGTTTGCATAGGCTACTGAGAG
SFN R56A-Forward	GGCCAGGCAGCTGCCTGGAGGGTG
SFN R56A-Reverse	GGCAGCTGCCTGGCCGCCCACCAC
SFN R129A, Y130A-Forward	TACTACGCAGCACTGGCCGAGGTGGCC
SFN R129A, Y130A-Reverse	GGCCAGTGCTGCGTAGTAGTCACCCTT

2-8 Proliferation assay

For analysis of cellular proliferation activity, a WST-1 (colorimetric) kit

(Roche Diagnostic, Mannheim, Germany) was used in accordance with the manufacturer's protocol after siRNA transfection.

2-9 Apoptosis assay

After siRNA transfection for 48 h, all cells containing dead cells and lived cells were collected after trypsinization. The positive control for apoptosis analysis was cells treated with 10 μM camptothecin (Sigma-Aldrich) for 24 h before collecting cells. The negative control was a lysate of viable non-treated PL16T cells. All cells were washed with 1x PBS and centrifuged at 5000 rpm for 6 min at 4°C, twice. The supernatants were completely removed and the cell pellets were lysed with M-PER containing protease and phosphatase inhibitor. The lysates were centrifuged for 15,000 rpm for 10 min at 4°C and the supernatants were used for Western blot analysis. Anti-caspase3 and anti-cleaved caspase3 antibodies from Cell Signaling Technology were used for evaluation on apoptosis.

2-10 Wound healing assay

PL16T cells were transfected with siUSP8 or siSFN for 48 h in10 cm dish and trypsinized cells to transfer to 12-well plate to obtain confluent cells in the plate (n=4). After 24 h, confluent cells were wounded by manual scratching with 200 μl pipette tips, washed with PBS, and incubated 37°C. The observation was performed 0, 3, 6, and 12 h after scratching but the wound was started to heal from 12 h and captured at 0 and 12 h.

2-11 Quantitative real-time PCR analysis

To confirm the transfection efficiency and change in the *EGFR* and *MET* gene expression level affected by USP8 or SFN knockdown, PL16T cells were evaluated using quantitative real time RT-PCR. Total RNA was prepared from siUSP8 or siSFN-transfected PL16T using the RNeasy Mini Plus Kit (QIAGEN) and the quality was evaluated using an Agilent 2100 Bioanalyzer (Thermo Fisher Scientific) as described above. One microgram of total RNA per 20 μl of the reaction mixture was converted to cDNA using a High Capacity cDNA Reverse Transcription Kit (Thermo Fisher Scientific). Quantitative real time PCR was performed with SYBRVR Premix Ex TaqTM (Perfect Real Time; Takara Bio, Shiga, Japan) on a GeneAmpVR 7300 Sequence Detection System (Thermo Fisher Scientific) in accordance with the manufacturer's protocol.

Primer for real-time PCR

USP8-Forward	CCTTTGACAAGAGCACGAAGTGAA
USP8-Reverse	ACATATGAACAGTGTTGGTGGGTGA
SFN-Forward	TCCACTACGAGATCGCCAACAG
SFN-Reverse	GTGTCAGGTTGTCTCGCAGCA

2-12 Western blot analysis

Total proteins were prepared on ice using Mammalian Protein Extraction Reagent (M-PER; Thermo Fisher Scientific) for cultured cells or Tissue Protein Extraction Reagent (T-PER; Thermo Fisher Scientific) for fresh tissue containing a Halt protease and phosphatase inhibitor cocktail (Thermo Fisher Scientific). The lysates were centrifuged and the insoluble fraction was discarded. The total protein in the soluble lysates was measured using a BCA protein assay kit (Thermo Fisher Scientific). Total protein aliquots (20 μg) were mixed with 5x sample loading

buffer supplemented with DTT, denatured at 95°C for 5 min, and electrophoresed on 10% or 12% Mini-PROTEAN TGX Precast Gels (Bio-Rad Laboratories, Hercules, CA). Proteins were transferred to polyvinylidene difluoride membranes using an iBlot gel transfer system (Thermo Fisher Scientific). The blots were then blocked and probed with various antibodies. The antibodies used for Western blot analysis were obtained from various commercial sources as follows: USP8, phosphor-EGFR (Tyr1045), phosphor-EGFR (Tyr1068), phosphor-MET (Tyr1003), phosphor-Akt (Ser473), Akt, phosphor-ERK1/2 (Thr202/Tyr204), ERK1/2, phosphor-STAT3 (Tyr705), STAT3, Myc, p14-3-3 binding motif, and Flag from Cell Signaling Technology (Denvers, MA); EGFR and GFP from Medical & Biological Laboratories (Aichi, Japan); MET and SFN from Immuno-Biological Laboratories (Fujioka, Japan); HA from Roche Diagnostics; and β-actin from Sigma-Aldrich. After extensive washing, immunoreactivity was detected with specific secondary antibodies conjugated to horseradish peroxidase (Thermo Fisher Scientific). Protein bands were visualized using SuperSignal West Femto Maximum sensitivity substrate (Thermo Fisher Scientific) and images were captured on a ChemiDoc Touch Imaging System (Bio-Rad Laboratories).

2-13 Co-immunoprecipitation (Co-IP)

A549 cells were used for endogenous two proteins interaction by Co-IP. Since PL16T cells were difficult to detect endogenous interaction, the cells were transfected with appropriate plasmids before 24 h of protein extraction. The total protein was extracted using IP Lysis Buffer (Thermo Fisher Scientific) containing a Halt protease and phosphatase inhibitor cocktail (Thermo Fisher Scientific). The cell extracts were concentrated using Amicon Ultra 3k (Merck Millipore, Billerica, MA) by centrifugal filtration, supplemented with an appropriate antibody

and 40 μl of washed protein A magnetic beads (Cell Signaling Technology), and incubated at 4°C overnight. The beads were subsequently pelleted on a magnetic separation rack for 15 s and washed 3 times using IP Lysis Buffer. The samples were then boiled at 95°C for 5 min to elute the immunocomplexed proteins. Levels of proteins in the elution products were assessed by Western blot analysis using the appropriate antibodies.

2-14 Immunofluorescence (IF)

The PL16T cells were plated on collagen-coated cover slides (Iwaki Biosciences, Tokyo, Japan) and fixed with 10% formalin. For immunofluorescence analysis, PL16T cells were incubated with appropriate antibody for 1 h at room temperature. After incubation with Alexa Fluor 488-labeled secondary antibody (Santa Cruz Biotechnology, Dallas, TX) or Alexa Fluor 594-labeled secondary antibody (Cell Signaling Technology) for 1 h at room temperature, the cells were analyzed using a fluorescence microscope (Biorevo BZ-9000; Keyence, Osaka, Japan).

The primary antibodies used for IF were obtained from various commercial sources as follows: anti-USP8 rabbit monoclonal antibody, anti-EEA1 rabbit monoclonal antibody from Cell signaling Technology, anti-LAMP1 mouse monoclonal antibody from Abcam, and anti-SFN rabbit polyclonal antibody from Immuno-Biological Laboratories, and anti-SFN mouse monoclonal antibody from Sigma-Aldrich.

2-15 Detection of ubiquitinated proteins with Co-IP

PL16T cells were transfected with siRNA for 24 h followed by HA-ubiquitin for 24 h. After transfection, the cells were treated with 25 mM NH_4Cl, a lysosomal inhibitor or 10 μM

MG132, proteasome inhibitor, for 4 h or 6 h, respectively at 37°C in a 5% CO_2 incubator. The total protein was extracted using IP Lysis Buffer (Thermo Fisher Scientific) containing a Halt protease and phosphatase inhibitor cocktail (Thermo Fisher Scientific) and 10 mM N-ethylmaleimide (NEM; Sigma-Aldrich), a deubiquitinase inhibitor. The cell extracts, containing 0.5 mg of total protein, were supplemented with an appropriate antibody with 40 μl washed protein A or G magnetic beads (Cell Signaling Technology) and incubated at 4°C overnight. The beads were subsequently pelleted on a magnetic separation rack for 15 s and washed 3 times using IP Lysis Buffer. The samples were then boiled at 95°C for 5 min to elute the immunocomplexed proteins. The ubiquitinated proteins in the elution product were assessed by Western blot analysis using the appropriate antibodies.

2-16 Detection of accumulated proteins at lysosome with IF

After siRNA transfection for 48 h, the cells on collagen-coated cover slides (Iwaki Biosciences, Tokyo, Japan) were treated with 25 mM NH_4Cl, a lysosomal inhibitor for 4 h at 37°C in a 5% CO_2 incubator and fixed with 10% formalin. For detection of ubiquitinated proteins with immunofluorescence, PL16T cells were incubated with anti-EGFR (Medical & Biological Laboratories) or anti-MET (Cell signaling Technology), and together with anti-LAMP1 (Abcam, Cambridge, MA) antibody for 1 h at room temperature. After incubation with Alexa Fluor 488-labeled secondary antibody (Santa Cruz Biotechnology, Dallas, TX) or Alexa Fluor 594-labeled secondary antibody (Cell Signaling Technology) for 1 h at room temperature in dark condition, the cells were analyzed using a fluorescence microscope (Biorevo BZ-9000; Keyence, Osaka, Japan).

2-17 Flow cytometry analysis

Expression of EGFR and MET at the cell surface was determined by plating the cells in 6-well plates at 48 h after siRNA transfection. The culture medium was replaced with serum-free medium for 16 h to block endocytosis of EGFR and MET. The cells were washed with PBS, detached with trypsin, and collected into tubes containing complete media on ice. The cells were washed twice with PBS containing 2% bovine serum albumin (BSA). The cells were incubated with phycoerythrin-conjugated (PE) monoclonal mouse IgG1 anti-EGFR (BioLegend, San Diego, CA), PE-conjugated monoclonal mouse IgG1 anti-MET (R&D Systems, Minneapolis, MN), or PE-conjugated anti-mouse IgG1 as an isotype control (BioLegend) on ice for 1 h in the dark. After two washes with PBS containing 2% BSA, the samples were analyzed with the BD FACSuite (BD Bioscience, San Jose, CA). Forward scatter/side scatter gating identified living cells.

2-18 Cyclohexamide chase assay

To block further protein biosynthesis of EGFR or MET, siRNA transfected PL16T cells were incubated in MCDB 153 HAA medium with 10 μg/ml cycloheximide (CHX; Sigma-Aldrich) for time-course. After CHX treatment, the cell lysates were analyzed by Western blot analysis.

2-19 Pulse-chase assay

Pulse-chase assay was modified from previous study (38). After transfection of siUSP8 or siSFN for 48 h in 10 cm collagen-coated dish, the cells were washed by PBS and incubated

with prewarmed DMEM medium without Met/Cys for 30 min at 37°C in a 5% CO_2 incubator. For the pulse radioisotope, the cells were labeled with ^{35}S-Met/Cys (10 μCi/ml) in DMEM medium without Met/Cys for 30 min at 37°C in a 5% CO_2 incubator. This pulse-labeling step was used to label newly synthesized protein. The pulse was followed by a chase in which cells are further incubated with the unlabeled counterpart of the precursor used for labeling. For the chase labeled-protein, the metabolic labeled cells were washed with culture medium for 3 times and incubated with culture medium in time course 0, 2, 5, and 10 h. After chasing, the cells were washed once and the total protein was extracted by IP Lysis Buffer (Thermo Fisher Scientific) containing a Halt protease and phosphatase inhibitor cocktail (Thermo Fisher Scientific). The radioisotope-labeled EGFR proteins were isolated from other cellular proteins by IP and performed Western blot analysis. For quantitative determination of proteins, the membrane containing the radioisotope-labeled EGFR was scanned β–ray using Typhoon FLA7000 (GE Healthcare, Chicago, IL) image analyzing system.

2-20 Statistical analysis

Group results are expressed as mean ± SD. Data were compared between groups using the *t* test to calculate 2-tailed distributions and a paired *t* test. Differences at P *<0.05, **<0.01, and ***<0.001 were considered significant. SPSS 22 statistical software (SPSS, Chicago, IL) was used for IHC data analysis as follows. Correlations of clinicopathological features with USP8 or SFN expression were analyzed using the chi-squared test. Disease-free survival according to USP8 or SFN expression was examined using the Kaplan-Meier method, and the significance of differences between survival curves was evaluated using log-rank test.

3. Results

3-1 Overexpression of USP8 and SFN in lung adenocarcinoma tissues

USP8 and SFN are highly expressed in human lung adenocarcinoma tissues.

To evaluate the expression pattern of USP8 and SFN in human lung adenocarcinoma tissue, immunohistochemistry (IHC) was performed using 193 cases. Both USP8 and SFN were stained in the cytoplasm of formalin-fixed paraffin-embedded (FFPE) specimens from surgically resected lung adenocarcinoma, and that the expression was higher in tumor tissue than in normal lung tissue (Fig. 6A-6D). Consistent with the IHC results, Western blot analysis revealed that USP8 and SFN were highly expressed in tumor tissue relative to normal lung tissue (Fig. 6E).

USP8 and SFN show correlative expression in human lung adenocarcinoma tissues.

To understand USP8 and SFN correlation in lung adenocarcinoma, USP8 and SFN both positive and both negative cases of IHC were divided. USP8 and SFN showed similar expression patterns in same localization of cytoplasm (Fig. 7A), and their expression was significantly correlated in 144/193 cases (74.6%, Fig. 7B).

Expression of SFN is associated with patient's prognosis.

Expression of SFN was significantly associated with gender, Noguchi classification, pathological subtype, pathological stage, lymphatic permeation, and vascular invasion. Unlike SFN, USP8 expression was significantly associated with only the Noguchi classification for

small adenocarcinomas of the lung (2 cm or less in diameter, Table 1). Moreover, SFN positivity was significantly associated with a poorer outcome relative to SFN-negative cases (p=0.007, Fig. 8B), whereas USP8 positivity was not (p=0.974, Fig. 8A).

Mutation in USP8 is not found in lung adenocarcinoma tissues.

USP8 has 14-3-3 binding motif, which plays critical regulation roles. To investigate mutation in 14-3-3 binding motif of USP8, pyro-sequencing analysis was performed using lung adenocarcinoma cell lines and pair of fresh human normal and tumor lung tissues. Unlike Cushing's disease (39), all cell lines including immortalized AIS cells and advanced stage lung adenocarcinoma cells and human lung tissue including normal and tumor had wild-type sequence of USP8 (Fig. 9).

3-2 Functional analysis of USP8 and SFN in lung adenocarcinoma cells

Selection of siRNA targeting USP8 or SFN in lung adenocarcinoma cells.

To determine the best siRNA targeting USP8 or SFN for functional analysis, three different kinds of siRNAs were transfected into the A549 cells. All of the siRNAs successfully suppressed the expression of USP8 or SFN both at mRNA (Fig. 10A and 10D) and protein level (Fig. 10B and 10E). As siUSP8-I and siSFN-I showed the most marked suppression of cellular proliferation, they were selected and used for further analysis (Fig. 10C and 10F).

Knockdown of USP8 or SFN decreases cellular proliferation in lung adenocarcinoma cells.

To evaluate whether USP8 and SFN regulate cellular functions including cellular proliferation and apoptosis, siRNA-USP8, SFN, or a scrambled control (siCON) were transfected in immortalized AIS cells, PL16T and lung adenocarcinoma cell lines harboring EGFR mutation, PC9 and H1975. Knockdown of USP8 or SFN significantly reduced the proliferation of all lung adenocarcinoma cells harboring EGFR mutation, similarly to A549 cells (Fig. 11). Since PL16T was the most effective reduction of cellular proliferation in knockdown of USP8 or SFN, PL16T cells were chosen for further functional assays (Fig. 11).

Knockdown of SFN or USP8 induces apoptosis in PL16T.

To examine reduction of proliferation was caused by induction of apoptosis, alteration of cleaved caspase 3, which is a representative apoptotic protein, was analyzed by Western blot analysis. Correlated with proliferation result, knockdown of USP8 or SFN in PL16T cells led to induction of apoptosis (Fig. 12A). Moreover, to investigate migration effect of knockdown of USP8 or SFN, wound healing assay was examined. Unlike SFN, knockdown of USP8 delayed recovery of scratch compared with siCON, indicating that USP8 regulates migration in PL16T cells (Fig. 12B).

3-3 USP8 regulates RTKs and SFN expression in lung adenocarcinoma cells

USP8 interacts both RTKs and SFN in lung adenocarcinoma cells.

USP8 has been reported to regulate RTKs such as EGFR and MET in advanced lung

adenocarcinoma cells (21). To confirm the interaction between USP8 and RTKs in A549 with high expression of SFN, co-IP was performed and USP8 interacted with SFN and RTKs such as EGFR and MET (Fig. 13A). Endogenous interaction between USP8 and RTKs as well as SFN was difficult to detect in PL16T cells. However, after overexpression of USP8, USP8 showed to interact with EGFR, and MET, but not with SFN due to low expression of SFN in PL16T cells (Fig.13B).

Overexpression of USP8 up-regulates EGFR expression in PL16T.

To investigate whether overexpression of USP8 regulates RTKs and SFN expression, Western blot analysis was performed in PL16T cells. Overexpression of USP8 increased EGFR expression but did not alter MET and SFN expression. Among downstream signaling factors, pAKT was slightly increased by overexpression of USP8 (Fig. 14)

Knockdown of USP8 down-regulates RTKs and SFN expression by posttranslational modification in PL16T.

To understand the function of USP8 in PL16T cells, siRNA-USP8 was transfected and the expression levels of SFN, RTKs, and their downstream factors were examined. Knockdown of USP8 down-regulated the level of SFN protein (Fig. 15A). Moreover, knockdown of USP8 decreased the expression of RTKs such as EGFR, pEGFR Y1068 (cellular proliferation-related phosphorylation site), and MET, and mainly decreased STAT3 and AKT signaling, in accordance with the results of the cellular proliferation assay (Fig. 15A).

Knockdown of USP8 down-regulates membrane surface of RTKs in PL16T.

Consistent with the results of Western blot analysis, surface EGFR and MET expressions were examined by flow cytometry. After serum starvation for excluding endosome RTKs, surface RTKs were directly stained with fluorescent conjugated antibody. Surface EGFR and MET were decreased significantly after USP8 knockdown (Fig. 15B and 15C). This is indicated that knockdown of USP8 regulates surface RTKs expression levels.

Knockdown of USP8 enhances ubiquitinated RTKs in PL16T.

To clarify whether knockdown of USP8 blocks recycling of RTKs, ubiquitinated EGFR and MET for RTK degradation were examined using co-IP after transfection with siRNA-USP8. Ubiquitinated EGFR and MET were detected after treatment with the lysosomal inhibitor, NH_4Cl, for 4 h to evaluate the accumulation of ubiquitinated proteins at lysosomes. Knockdown of USP8 strongly induced accumulation of poly-ubiquitinated EGFR and MET, as revealed by Western blot analysis (Fig. 16).

Knockdown of USP8 accumulates ubiquitinated RTKs at lysosome in PL16T.

To investigate where ubiquitinated EGFR and MET increase in the cell, IF under treatment of lysosomal inhibitor, NH_4Cl was performed and showed co-localization of EGFR and MET at lysosomes that were immunostained with antibody against LAMP1, a lysosomal marker (Fig. 17A and 17B). Consist with ubiquitinated EGFR or MET in co-IP results, knockdown of USP8 enhanced accumulation of EGFR and MET at lysosome for their degradation.

3-4 SFN regulates RTKs and USP8 expression in lung adenocarcinoma cells

SFN interacts both RTKs and USP8 in lung adenocarcinoma cells.

A previous study using co-IP/MS analysis had identified various SFN binding partners, including EGFR, in nasopharyngeal carcinoma (40). To investigate SFN binding with RTKs in lung adenocarcinoma cells, co-IP was performed. As had been shown previously, endogenous SFN was found to interact with USP8 and RTKs including EGFR and MET in A549 cells (Fig. 18A). Since endogenous interaction between SFN and RTKs was difficult to detect in PL16T, SFN plasmid was transfected to PL16T cells, which immortalized AIS cell line showed low expression of SFN. Overexpression of SFN was shown interaction with EGFR or MET, but not with USP8 (Fig. 18B).

Overexpression of SFN up-regulates EGFR expression in PL16T.

To investigate whether overexpression of SFN regulates RTKs and USP8 expression, Western blot analysis was performed in PL16T cells. Similarly to overexpression of USP8, overexpression of SFN increased EGFR and USP8 expression but did not alter MET. Among downstream signaling factors, pSTAT3 and pERK was increased by overexpression of SFN (Fig. 19).

Knockdown of SFN regulates RTKs and USP8 expression in PL16T.

To demonstrate that SFN regulates the expression of USP8 and RTKs, PL16T cells were transfected with siRNA-SFN. Knockdown of SFN increased the total expression of EGFR protein, whereas total MET and downstream factors such as pSTAT3 were decreased (Fig. 20A). RTKs have various phosphorylation sites, which operate in degradation- or cellular proliferation-related signaling. Whereas pEGFR Y1068 is associated with cellular proliferation, EGFR and MET also contain phosphorylation sites at Y1045 and Y1003, respectively, where c-Cbl, E3 ligase conjugates ubiquitin, leading to protein degradation. I found that pEGFR Y1045 and pMET Y1003 showed higher after SFN knockdown than control (Fig. 20A), indicating that knockdown of SFN strongly induces degradation signaling of RTKs. The up-regulation of total EGFR after transfection with siRNA-SFN might be explained by an increase of pEGFR Y1045, which is destined for degradation.

SFN directly regulates and stabilizes USP8 expression in PL16T.

A rescue experiment revealed that the reduction of USP8 expression after SFN knockdown was abrogated by overexpression of SFN (Fig. 20B), indicating that SFN directly regulates the expression of USP8 protein. As supportive evidences for that SFN stabilizes USP8 expression, knockdown of SFN enhanced accumulation of poly-ubiquitinated USP8, which is indicated by higher molecular size of original with smear band, under treatment of MG132, a proteasome inhibitor, for 4 h in time-dependent manner (Fig. 20C).

Knockdown of SFN accumulates ubiquitinated RTKs at lysosome in PL16T.

Next, to demonstrate whether SFN is involved in degradation of RTKs, similarly to USP8, ubiquitinated EGFR or MET were detected in PL16T under treatment of lysosomal inhibitor,

NH_4Cl. Expression of ubiquitinated EGFR and MET after knockdown of SFN was clearly higher than in the controls (Fig. 21). Knockdown of SFN induced the accumulation of EGFR and MET at lysosomes that were immunostained with antibody against LAMP1, a lysosomal marker, being destined for degradation (Fig. 22)

Knockdown of SFN reduced half-life of RTKs in PL16T.

Consistent with the fact that knockdown of SFN regulates RTKs expression, the half-life of EGFR and MET after knockdown of SFN was shorter than in controls treated with CHX in PL16T cells (Fig. 23A). Notably, EGFR expression in siSFN was higher expression at 0 h but more quickly decreased until 12 h compared with siCON. To confirm this result, pulse-chase assay for EGFR using radioisotope was implemented. Consistent with CHX chase assay, knockdown of SFN quickly removed radioisotope labeled EGFR (Fig. 23B).

3-5 SFN and USP8 collaboratively regulate RTKs expression in lung adenocarcinoma cells

USP8 specifically interacts with SFN among 14-3-3 proteins at endosome in PL16T.

Previous studies have found that USP8 interacts with 14-3-3 proteins in embryonic murine brain (41) and T-cells (42), but not in lung. To clarify whether USP8 binds specifically to SFN in lung, co-IP was carried out to examine the interaction of USP8 with SFN, 14-3-3 epsilon, or 14-3-3 zeta, separately. Unlike previous observations, the results indicated that among three kinds of 14-3-3 proteins, only SFN bound specifically to USP8 in PL16T cells (Fig. 24). In addition, IF results were shown that USP8 and SFN were co-localized in the cytoplasm,

particularly in both the early and late endosome, in PL16T cells (Fig. 25). These data indicate that USP8 interacts with SFN in endosomes.

Mutation of 14-3-3 binding motif in USP8 impairs interaction with SFN and down-regulates expression of RTKs and their downstream factors in PL16T.

The 14-3-3 binding motif of USP8 (RSYSSP) is essential in order for USP8 to interact with the 14-3-3 family, and S718 of the 14-3-3 binding motif in USP8 is a critical biological phosphorylation site (Fig. 4) (39). To elucidate whether SFN regulates USP8 activity in RTK recycling, a mutant form of USP8, S718C, was generated which shows impaired binding with SFN. Co-IP was performed after overexpression of either the wild-type or mutant USP8 to examine the resulting interaction with SFN. The interaction of the mutant USP8 with SFN was obstructed, and phosphorylation at the S718 residue was also lost (Fig. 26A), signifying that phosphorylation of USP8 at this site is crucial for SFN binding.

Moreover, PL16T cells were transfected individually with the wild-type USP8, the mutant USP8 S718C, and the mutant USP8 C786S, which has a point mutation in the catalytic domain causing inactivation of deubiquitination. As expected, the mutant USP8 S718C decreased the expression of RTKs including EGFR and MET as well as downstream factors including pAKT and pSTAT3, in comparison with the wild-type USP8 (Fig. 26B).

Collectively, these findings suggest that binding of SFN with USP8 is essential for deubiquitination of RTKs in PL16T cells.

Mutation of ligand recognition site in SFN impairs interaction with USP8 and negatively regulates RTKs in PL16T.

According to previous study, SFN has four important residues, Lys49, Arg56, Arg129, and Tyr130, for recognizing of phospho-target proteins such as USP8 in lung adenocarcinoma (10). These positive charged residues specifically interacts with negative charged phospho-Ser of ligands. To demonstrate whether these multiple four residues or single specific residue is required for SFN association with USP8, SFN mutants were generated multiple mutant and single mutant such as K49A, R56A, and R129A combined with Y130A, respectively and applied to co-IP. All mutants almost abolished interaction with USP8 (Fig. 27A and 27B). Because of impairment of binding with USP8 and SFN by mutation of biding sites, co-transfection of mutant USP8 and SFN decreased RTKs expression compared with co-transfection of wild-type USP8 and SFN (Fig. 27C and 27D). These results showed that the four residues of SFN are very responsible for USP8 association and SFN-USP8 complex plays an important regulation role of RTKs stabilization.

Phosphorylation of USP8 is regulated by Serine/Threonine kinase and phosphatase.

Panner A. *et. al*. has reported that enzymatic activity of USP8 is dependent on AKT, a serine/threonine-specific protein kinase (43). To reveal the involvement of AKT on regulation of USP8 phosphorylation on its 14-3-3 BM, A549 cells were treated with AKT inhibitor, LY294002. Treatment of LY294002 apparently decreased USP8 phosphorylation on 14-3-3 BM and also impaired binding of USP8 with SFN, showing that AKT is one of the key kinases for USP8 regulation (Fig. 28A). In contrast, specific phosphatase for USP8 is still unknown. As a best-known phosphatase with strong effect, we focused on PP1 or PP2a and treated cells with their inhibitor, okadaic acid. Expectedly, treatment of okadaic acid led to a marked increase of USP8 phosphorylation on 14-3-3 BM and binding of USP8 with SFN (Fig. 28B).

4. Discussion

In this study, immunohistochemically, both USP8 and SFN showed higher expression in lung adenocarcinoma than in normal lung tissue, and their expressions levels were mutually correlated in lung adenocarcinoma tissues (Fig. 6 and Fig. 7). Clinically, the level of SFN expression was associated with patient outcome, but that of USP8 is not (Table 1 and Fig. 8). This discrepancy will be explained that the biological effect of USP8 might be included in that of the multi-functional protein, SFN, and the expression of USP8 itself may not influence the final outcome.

Moreover, knockdown of SFN or USP8 similarly suppressed cellular proliferation and induced apoptosis in lung adenocarcinoma cell lines *in vitro* (Fig. 10 and Fig. 11). These phenomena were induced most markedly in the PL16T cell line, which was established from AIS, an extremely early-stage form of adenocarcinoma, in comparison with other cell lines derived from advanced adenocarcinoma (Fig. 11). Previous study had found that DNA demethylation-triggered abnormal overexpression of SFN is an early event in the malignant progression of lung adenocarcinoma similarly to genetic alteration of EGFR, K-RAS, and p16 (3, 11, 36). Since overexpressed SFN induces stabilization of USP8 protein (Fig. 19 and Fig. 20), alteration of USP8 might be also one of the oncogenic events induced by SFN at the early stage of lung adenocarcinoma.

As reported before, I confirmed that USP8 binds and regulates EGFR and MET to accelerate their deubiquitination (Fig. 13 and Fig. 16). Knockdown of USP8 suppressed the expression of EGFR, pEGFR Y1068 (a cellular proliferation-related site), MET, pSTAT3, and pAKT, and this effect was thought to be associated with the accelerated ubiquitination of EGFR and MET. After transfection with siRNA-USP8, membrane-associated EGFR and MET were

ubiquitinated and accumulated in lysosomes (Fig. 15 and Fig. 16-17). On the other hand, SFN was also shown to be a binding partner of EGFR and MET (Fig. 18), and knockdown of SFN suppressed the expression of MET and pSTAT3, although total EGFR did not show any suppression (Fig. 20). However, pEGFR Y1045 and pMET Y1003 (sites related to protein degradation) were upregulated and these phenomena indicated that knockdown of SFN strongly induced degradation signaling of EGFR and MET. The increase of EGFR expression in Fig. 20A due to suppression of SFN is thought to have been due to binding of SFN to the other binding partners, thus influencing EGFR expression. Additionally, I can not exclude the possibility that knockdown of SFN might lead to recovery of EGFR biosynthesis followed by a decrease of cell viability, as feedback regulation for cell survival.

Moreover, knockdown of USP8 or SFN increased the amount of ubiquitinated RTKs (Fig. 16 and Fig. 21). This similar phenomenon in knockdown of USP8 and SFN imply their functionally close association. Thus, I confirmed that USP8 is a unique binding partner of SFN, unlike other members of the 14-3-3 protein family (Fig. 24) and co-localized in early- and late-endosome (Fig. 25). Additionally, mutant USP8 S718C and mutant SFN, which are unable to bind to USP8 and SFN each other, impaired the stability of RTKs (Fig. 26 and Fig. 27). These findings lend support to the possibility that SFN promotes USP8 activity, causing RTK stabilization in lung adenocarcinoma.

Mizuno et al. and Dufner et al. have identified 14-3-3 epsilon, zeta, gamma, and beta, but not sigma (SFN), as USP8 binding partners (17, 42). 14-3-3 epsilon and beta, which are highly expressed in mammalian brain (6), inhibit USP8 activity in Cushing's disease (44-46) and mouse T-cells (42) by blocking the cleavage of USP8, leading to hyperactive deubiquitination of EGFR. Moreover, mutations of USP8 in Cushing's disease frequently occur at the 14-3-3 binding motif,

leading to up-regulation of EGFR and subsequent hyperproduction of ACTH, the hallmark of Cushing's disease (39). In contrast to Cushing's disease, any somatic mutation did not revealed at the 14-3-3 binding motif of USP8 in lung adenocarcinoma tissue, or any fragmentary form of USP8 in lung adenocarcinoma cells (Fig. 9).

Previous studies have indicated that each of the 14-3-3 member proteins has unique functions, which are context-dependent and also organ- or tissue-dependent (6). SFN in particular is evolutionarily distinct from all of the other 14-3-3 proteins from the viewpoint of sequence conservation (5), and shows the closest association with lung cancer (47). In this regard, abnormal activation of USP8 induced by SFN is a unique and tissue-specific phenomenon in lung adenocarcinoma.

Post-translational modification including ubiquitination and deubiquitination is the key mechanism for regulation of degradation mediated by cell surface receptors and ligands (13). USP8 directly deubiquitinates and consequently recycles RTKs to their lysosomal degradation, thereby maintaining oncogenic signaling (17, 23). USP8 enzymatic activity is dependent on phosphorylation by c-Src, a non-receptor tyrosine kinase (48), and AKT, a serine/threonine-specific protein kinase (43). Similarly, here we suggested that AKT and also several phosphatases might be involved in regulation of USP8 phosphorylation (Fig. 28). Since AKT is usually up-regulated in tumor cells because of various stimulation including RTKs stabilization through USP8 activation, it is possible that over-activation of AKT might accelerate binding of phospho-USP8 with SFN. Based on the fact that phospho-USP8 binds to SFN, overexpression of SFN in lung adenocarcinoma might promote interaction with USP8 via its phosphorylation and induce a conformational change in USP8 that increases its enzymatic activity and stability (8) (Fig. 29). Recently, a similar mechanism for regulation of USP8 was reported for Tiam1, a Wnt-

responsive gene, which is phosphorylated by AKT, allowing it to bind with 14-3-3 and thus rendering it stable, thereafter accumulating to promote cell growth and proliferation (49).

Many molecular targeting drugs have been developed for advanced lung adenocarcinomas harboring EGFR mutation or ALK rearrangement (50, 51). Although TKIs for EGFR and EML4-ALK suppress tumor cell growth and are initially very effective, most tumors subsequently aquire resistance to the drugs. Byun et al. reported that a USP8 inhibitor suppressed both growth and tumor formation by both TKI-resistant and -sensitive NSCLC cells, and suggested that USP8 might be a preferable theraputic target for overcoming aquired resistance (21). However, it would be expected that any USP8 inhibitor might dysregulate the physiological important functions of USP8 in normal tissues, causing severe side effects. On the other hand, SFN shows high tumor-specific expression and induces aberrant USP8 activation in lung adenocarcinoma. Therefore, a SFN inhibitor would be more a selective and desirable therapeutic target for lung adenocarcinoma than USP8, with the possibility of effectiveness against TKI-resistant tumors.

Low-dose CT screening trials have suggested that the number of adenocarcinomas detectable at an early stage, such as AIS and minimally invasive adenocarcinoma (MIA), has been increasing. In comparison to the standard treatments for advanced adenocarcinoma, no treatments for AIS and MIA, apart from surgical resection, have yet been established. Moreover, it is still being debated whether the use of surgery for AIS is a suitable approach, or whether it constitutes over-treatment. Here, I have shown that SFN regulates USP8 function, even in an AIS cell line, PL16T, *in vitro*. These results suggest that SFN holds promise as a therapeutic target for not only advanced, but also very early-stage lung adenocarcinoma.

5. Perspectives

Oncogenic function of SFN-USP8 complex and its application in diagnosis and treatment of lung adenocarcinoma

Abnormalities of plasma membrane receptors such as RTKs in cancer cells are widely acknowledged and known to cause overexpression of them. Moreover, lung adenocarcinoma is considered to progress in a stepwise manner with the different 5-year survival rate and various genetic alterations. Particularly, mutation of RTKs including EGFR or MET is one of the most important alteration arising from atypical adenomatous hyperplasia (AAH) or AIS, precancerous or early stage of lung adenocarcinoma.

However, most lung adenocarcinoma patients with poor prognosis harbor mutation of RTKs and undergo molecular targeted therapies in advanced stage. In this period, it is difficult to cure it completely, and most tumors acquire resistance to the drugs by second mutation of targeted proteins. Therefore, research focus had been changing to study and identify specific molecular target that can be applied for detection and treatment of at an early stage.

In the present study, I demonstrated the molecular mechanism underlying the binding of SFN to USP8 in lung adenocarcinoma cells, resulting in RTK stabilization. It is suggested that SFN is one of the target candidates for diagnosis and treatment of early stage lung adenocarcinoma.

A recent report was worthy of notice that SFN can be released into the extracellular environment physiologically through exosomes (52), which play important roles in cellular communication by containing diverse biomarkers implying cell condition, and the aberrant exosomal process was observed in various cancer cells including lung cancer (53, 54).

Generally, tumor cells can secrete more exosomes than normal cells, but more importantly, the content of exosomes from tumor cells is distinct, which has clinical significance (55). Exosomes produced by normal as well as tumor cells are released into extracellular space and present in all human body fluids including blood, urine, cerebrospinal fluid, and ascites (56). Therefore, SFN in exosomes can be an attractive and useful diagnostic biomarker for early-stage lung adenocarcinoma using body fluids such as serum or bronchoalveolar lavage.

6. Conclusions

Unlike the current treatment strategy for advanced adenocarcinomas, no therapeutic approach for early-stage lung adenocarcinomas such as AIS has yet been established, except surgical resection. SFN is a novel and unique oncogene that accelerates tumor initiation and early malignant progression of lung adenocarcinoma. In this study, I investigated the mechanism underlying the interaction of SFN with its binding partner protein, USP8, which contributes to stabilization of RTKs such as EGFR and MET through deubiquitination activity. SFN was shown that facilitates aberrant activation of USP8 and subsequently protects RTKs from lysosomal degradation in an AIS cell line. These new findings suggest that SFN may be central to the development of a useful therapeutic strategy for both early and advanced lung adenocarcinomas.

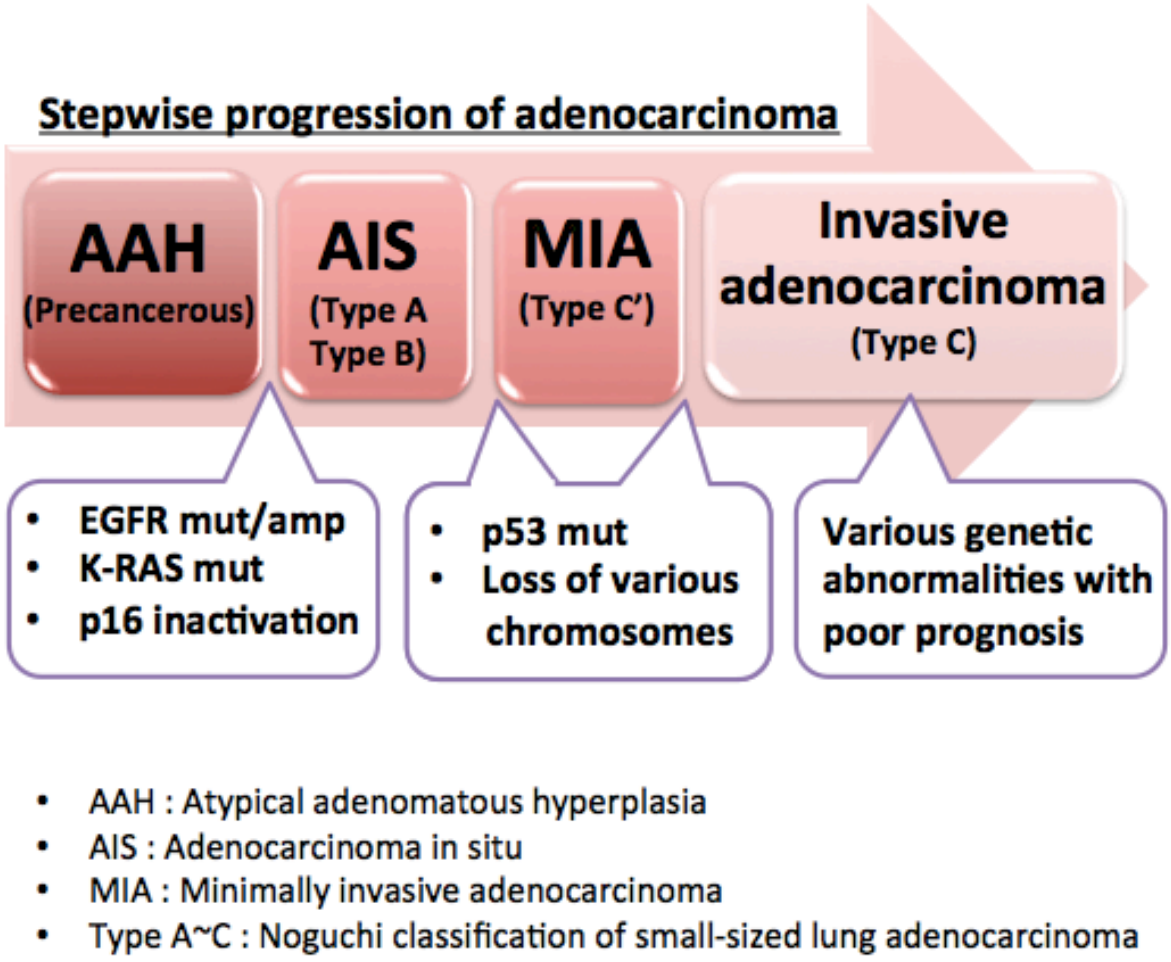

Fig. 1. Stepwise progression of adenocarcinoma with molecular alterations.

Noguchi classification is closely associated with stepwise progression of peripheral type adenocarcinoma, which is subcategorized into type A to C. Lung adenocarcinoma develops and progresses to invasive carcinoma through AAH, AIS, and MIA. The first period, AAH progresses to AIS, frequently occur gene mutation such as EGFR mutation or amplification, K-RAS mutation, and anti-apoptotic abnormality such as p16 tumor suppressor gene inactivation. The second period, AIS progresses to invasive adenocarcinoma, acquire various additional genetic alteration such as p53 mutation, allelic imbalances at 11p11-p12, 17p12-p13, and 18p11 (3).

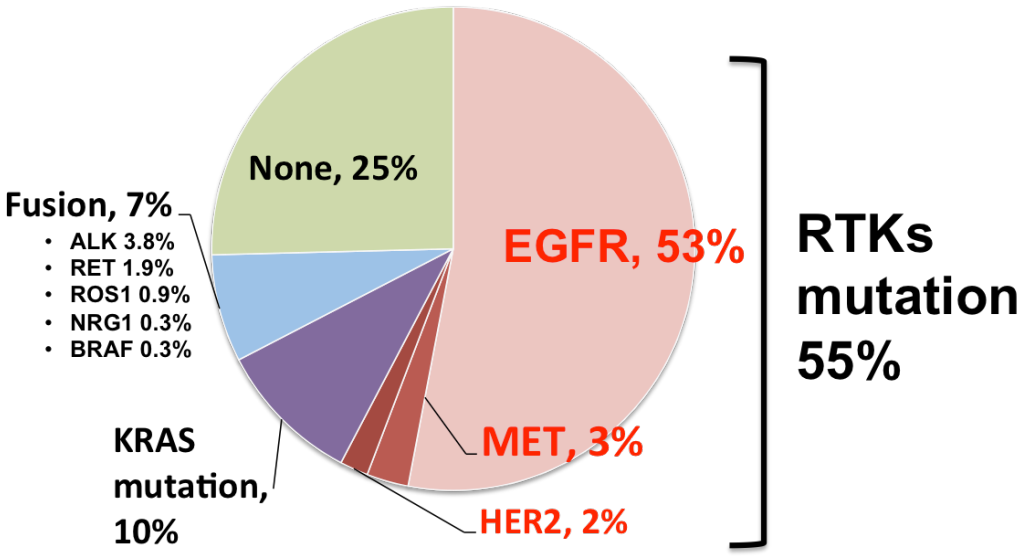

Fig. 2. Frequencies of driver oncogene aberrations in lung adenocarcinoma.

The data were obtained from a Japanese cohort (n=319) and modified from Saito M et. al. ,Cancer science, 2016, 107,6, 713-720.

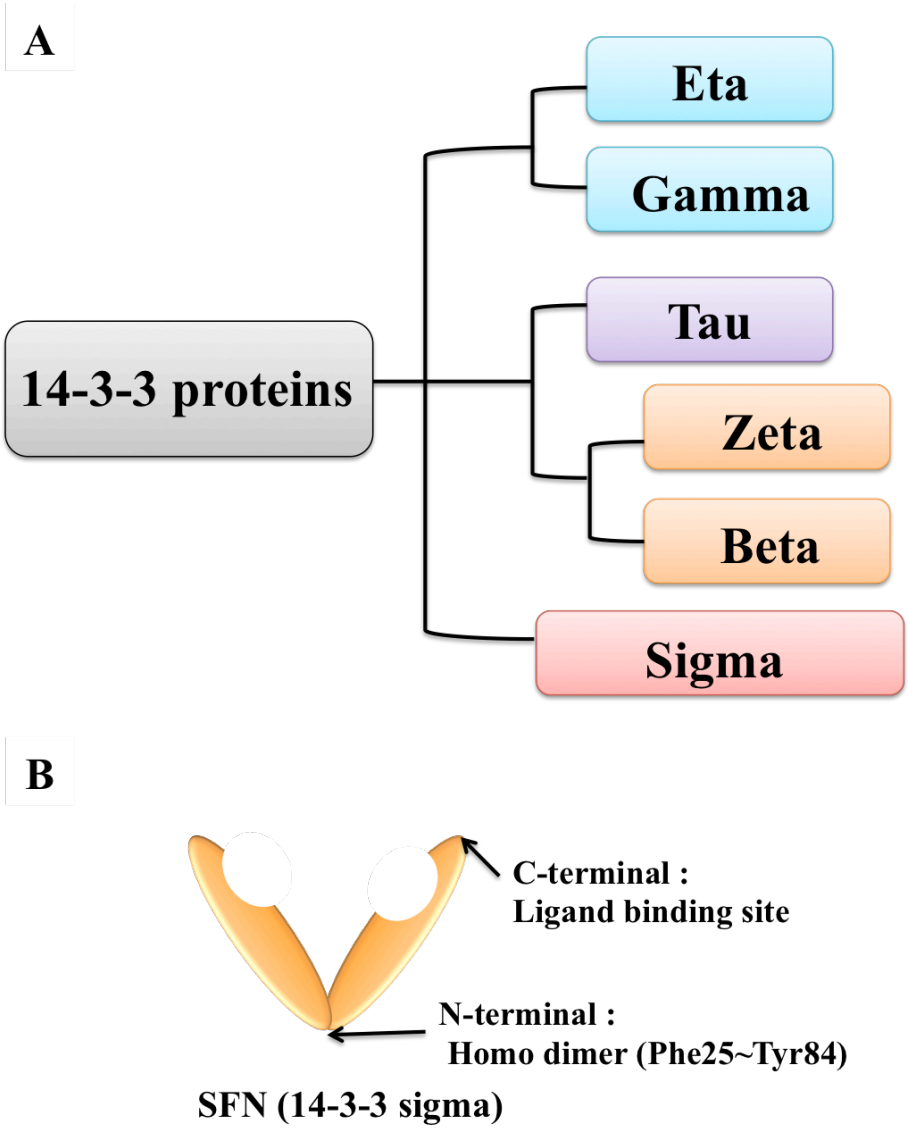

Fig. 3. 14-3-3 cladogram and SFN structure.

(A) 14-3-3 sigma (SFN) is evolutionarily distinct from clades encompassing all other 14-3-3 proteins (5). (B) SFN can be observed as homodimer form, which may be required for SFN function (10).

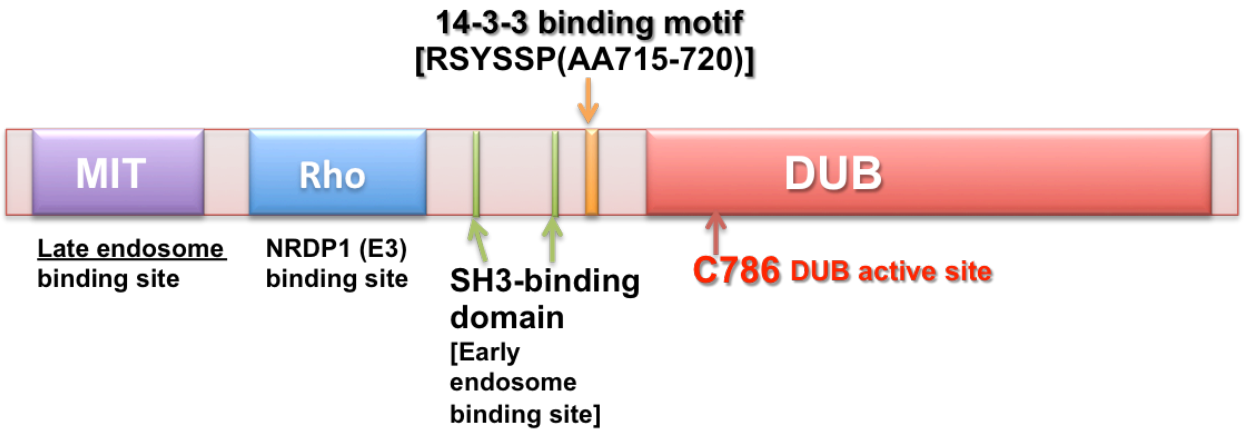

Fig. 4. Human USP8 protein structure.

The human USP8 has a theoretical molecular weight of 130 kDa and a pI of 8.7. USP8 contains a deubiquitinase catalytic (DUB) domain (residues 774-1106), a microtubule interacting and transport (MIT) domain (residues 8-137), a rhodanese-like (Rho) domain (residues 185-310), two Src homology 3-(SH3) binding domains (SH3-I residues, 405-413; SH3-II residues, 700-708), and 14-3-3 binding motif (residues 715-720). The function of USP8 deubiquitinase activity may be regulated by phosphorylation and by specific protein-protein interaction (57).

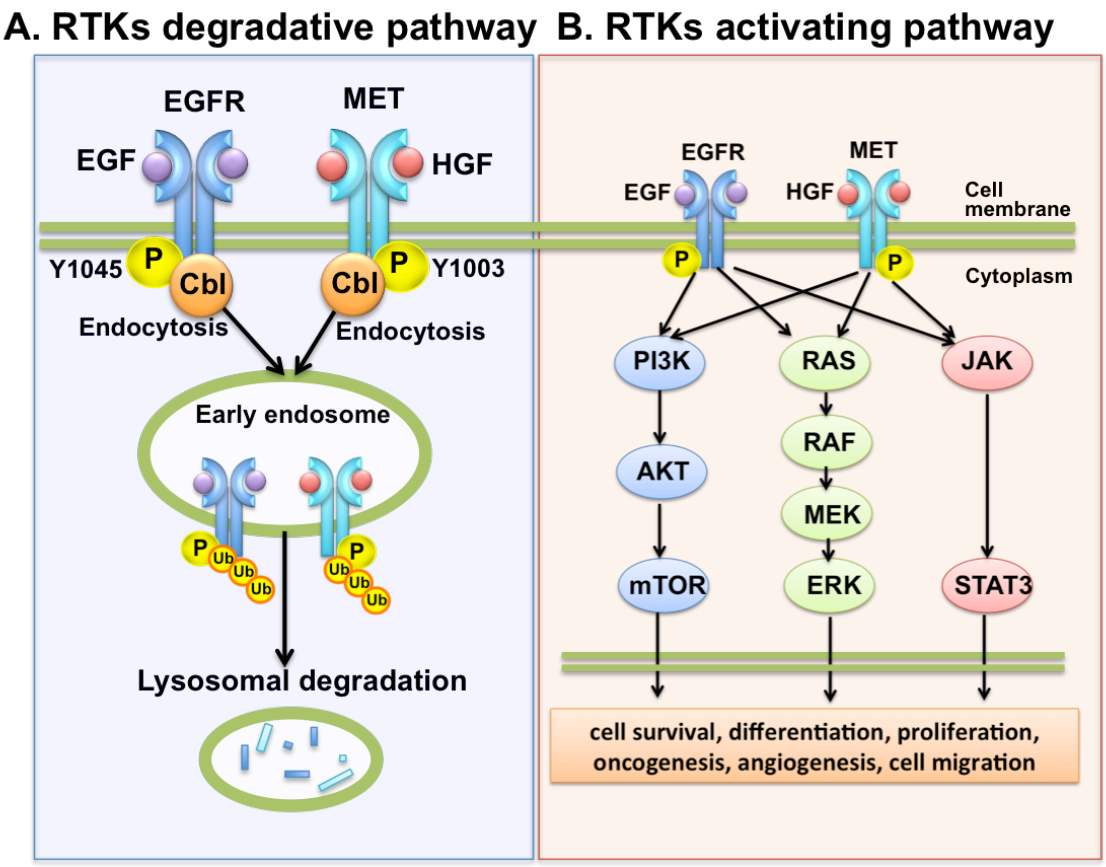

Fig. 5. RTKs signal transduction.

(A) Following ligand binding, RTKs such as EGFR and MET get activated and dimerized via phosphorylation. One phosphorylation site at Y1045 for EGFR and Y1003 for MET, serves a docking site for the ubiquitin ligase Cbl. The ubiquitinated RTKs are rapidly transported to early endosome by endocytosis process and eventually degraded at lysosome. This process is down-regulation pathway of RTKs. (B) On the other hand, RTKs also have another phosphorylation site such as Y1068 for EGFR and Y1234/Y1235to activate downstream signaling transduction, such as PI3K/AKT/mTOR, RAS/RAF/MEK/ERK, and JAK/STAT3, which are critical for cancer cell survival and proliferation (58, 59).

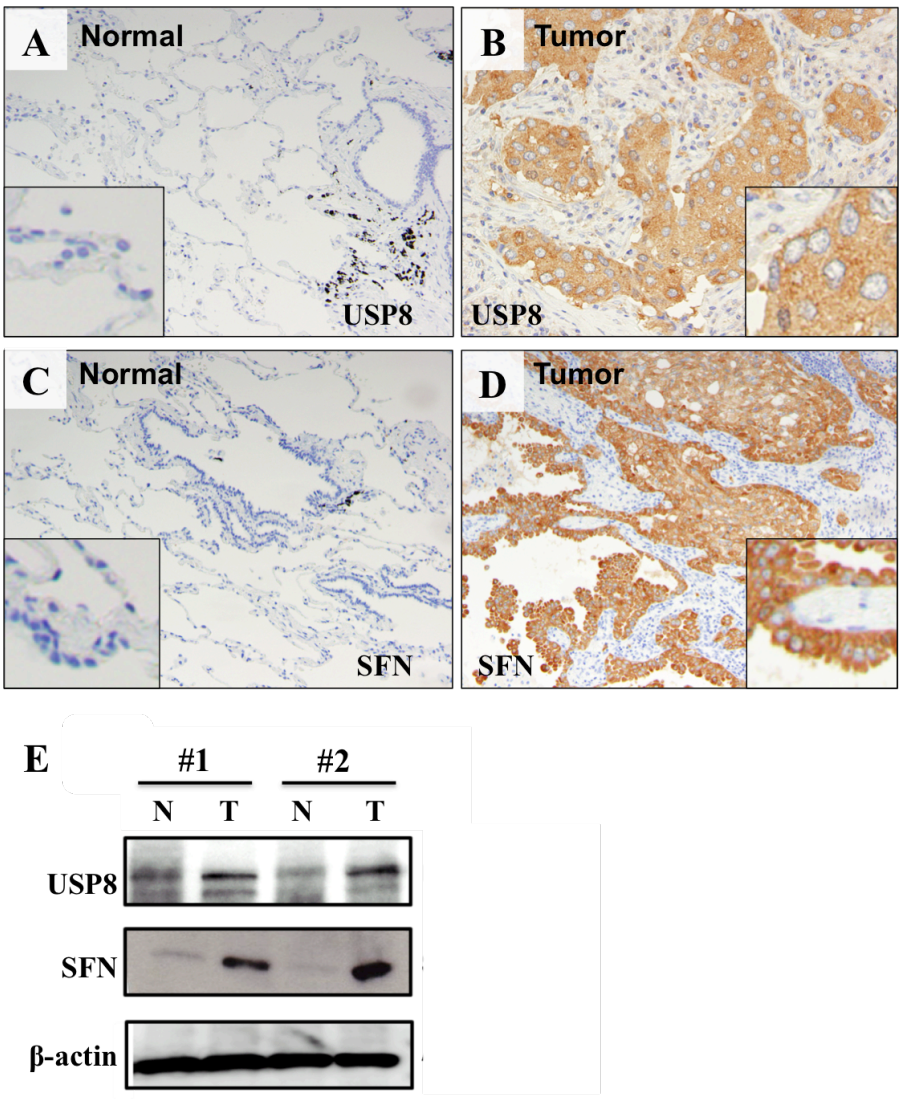

Fig. 6. The expressions of USP8 and SFN in tumor tissue.

(A-D) Immunohistochemistry (IHC) for USP8 and SFN was performed using formalin fixed and paraffin embedded (FFPE) specimens of 193 cases of surgically resected lung adenocarcinoma. Normal lung tissues were almost negative for USP8 (A) and SFN (C), whereas tumorous tissues showed higher expression of USP8 (B) and SFN (D) mainly in the cytoplasm. (E) Western blot analysis of fresh lung tissue demonstrated expression of USP8 and SFN in both normal and tumorous tissue, but the expression level in tumor was higher than normal. N, normal lung tissue; T, tumorous lung tissue; #1 and #2, case number.

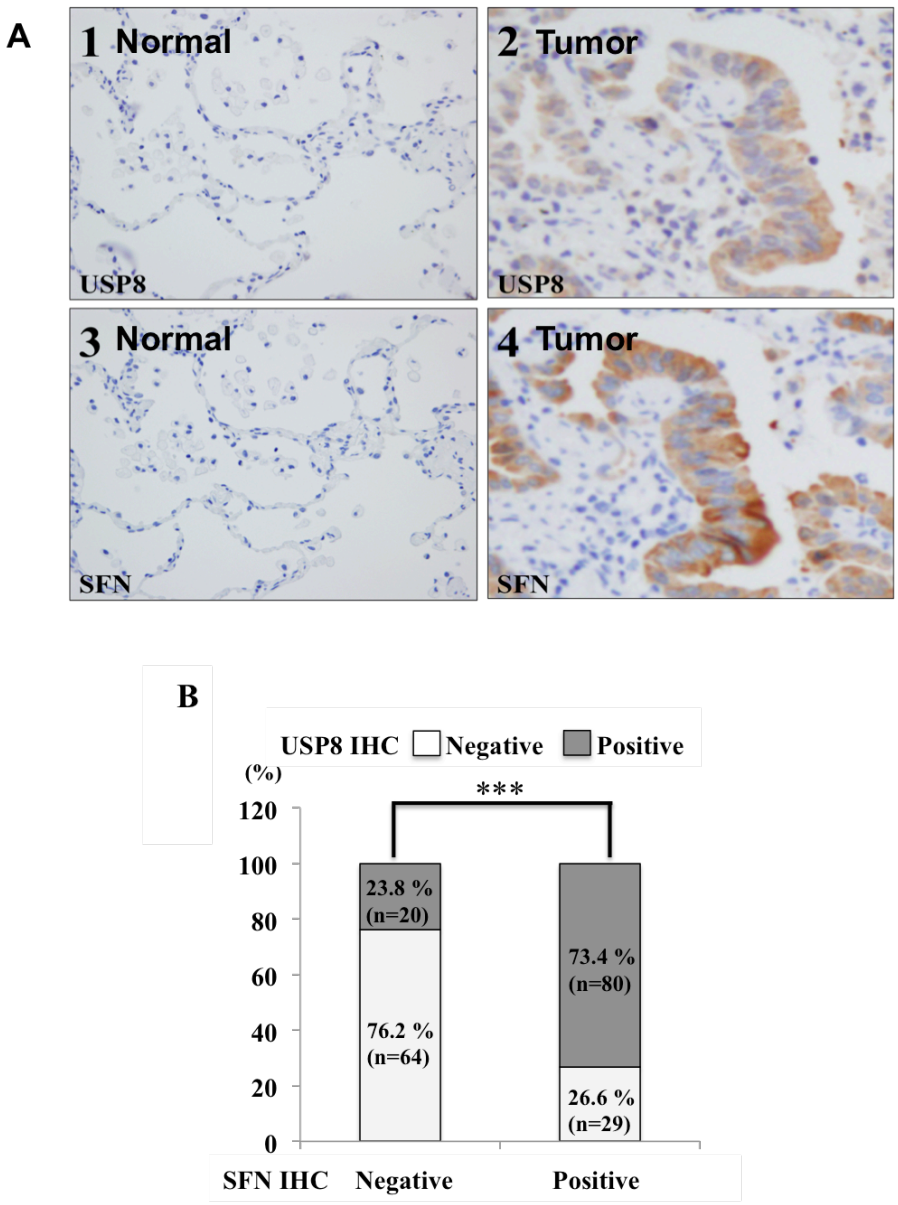

Fig. 7. USP8 and SFN show a corresponding increase of expression in human lung adenocarcinoma tissues.

(A) USP8 and SFN were detected mainly in the cytoplasm of the tumor cells with a similar staining pattern. Normal lung tissue was almost negative for USP8 (A-1) and SFN (A-3), whereas tumor tissue showed higher expression of USP8 (A-2) and SFN (A-4). (B) Correlation analysis of USP8 and SFN was performed using the IHC results. Correlated cases were significantly more than uncorrelated cases in USP8 and SFN IHC (chi-squared test, ***p<0.001).

Table 1. SFN or USP8 expression in relation to clinicopathological features of patients with lung adenocarcinoma.

Clinicopathological Features	SFN Expression		Total patients	*P*-value	USP8 Expression		Total patients	*P*-value
	Negative	Positive			Negative	Positive		
IHC	84	109	193		93	100	193	
Age (yr)				0.822				0.429
≤60	22	27	49		26	23	49	
>60	62	82	144		67	77	144	
Gender				0.032				0.191
Female	43	39	82	*	44	38	82	
Male	41	70	111		49	62	111	
Noguchi classification				0.003				0.039
Type A	8	0	8	**	8	0	8	*
Type B	9	6	15		7	8	15	
Type C'	6	3	9		5	4	9	
Type C	22	20	42		22	20	42	
Type D	5	10	15		6	9	15	
Type F	1	2	3		0	3	3	
Total	51	41	92		48	44	92	
Pathological Subtype				<0.001				0.313
AIS	19	6	25	***	17	8	25	
MIA	7	5	12		7	5	12	
Invasive adenocarcinoma								
Lepidic	18	31	49		19	30	49	
Acinar	10	11	21		9	12	21	
Papillary	13	13	26		13	13	26	
Micropapillary	2	2	4		3	1	4	
Solid	5	31	36		15	21	36	
IMA	10	10	20		10	10	20	
Pathological Stage				0.046				0.192
Stage I	65	65	130	*	64	66	130	
Stage II	9	24	33		11	22	33	
Stage III	10	18	28		17	11	28	
Stage IV	0	2	2		1	1	2	
Lymphatic permeation				0.004				0.413
Ly0	63	60	123	**	62	61	123	
Ly1	21	49	70		31	39	70	
Vascular invasion				<0.001				0.872
V0	63	50	113	***	55	58	113	
V1	21	59	80		38	42	80	

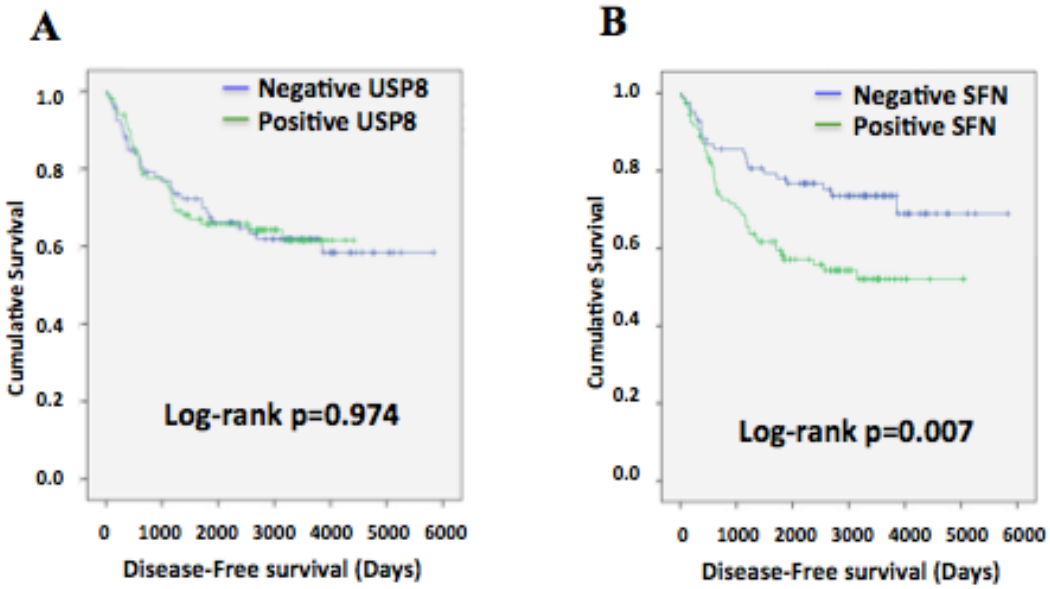

Fig. 8. SFN expression is associated with the outcome of the lung adenocarcinoma patients.

Disease-free survival (DFS) depicted as Kaplan-Meier curves showing the correlation between outcome and SFN or USP8 expression. Positive expression of SFN was associated with a poorer outcome than negative expression (p=0.007), but USP8 expression did not show the correlation (p=0.974).

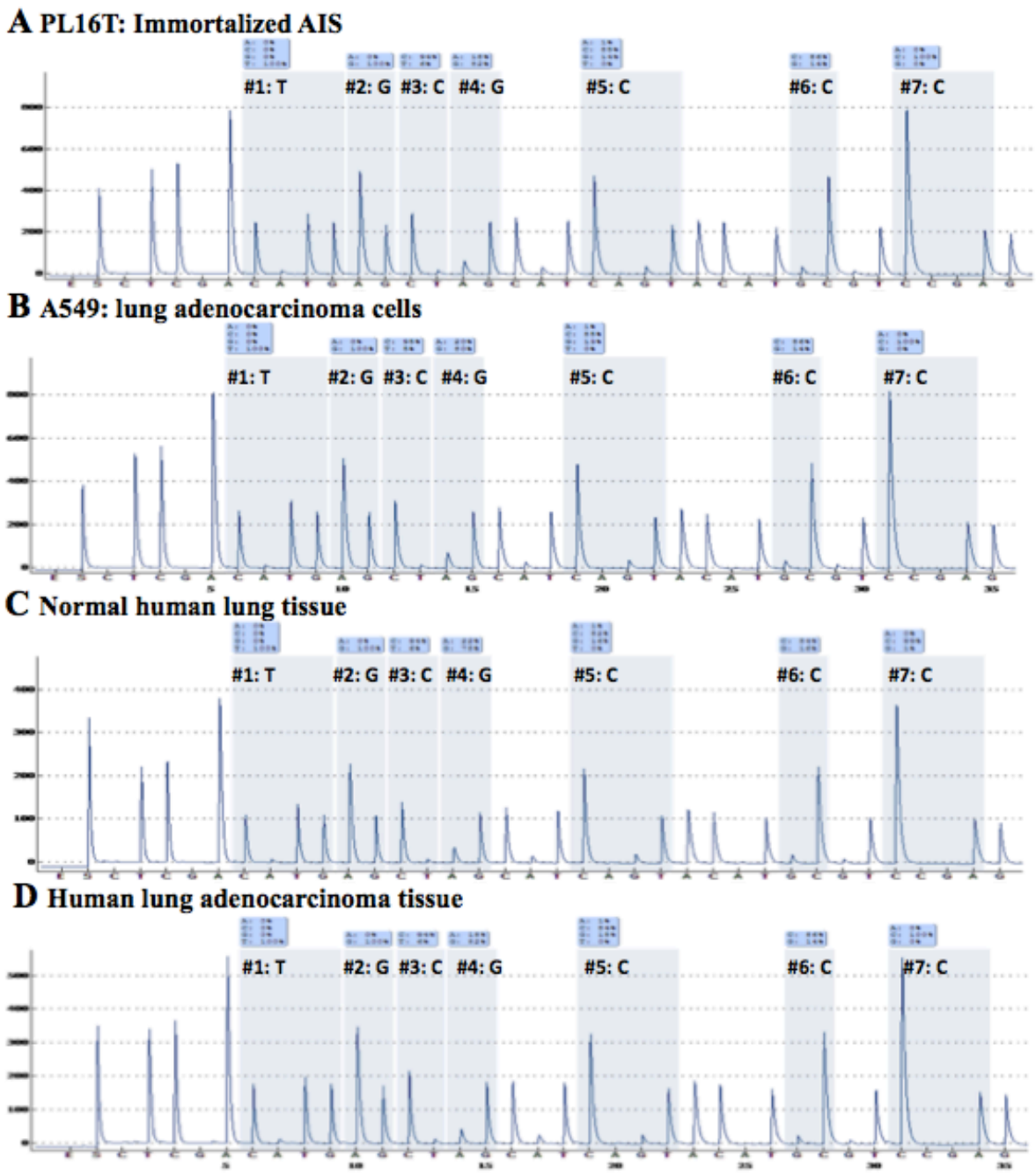

Fig. 9. Mutant of USP8 in 14-3-3 binding motif undiscovered in lung adenocarcinomas.

(A and B) Genomic DNA was extracted from the PL16T and A549 cell lines and (C and D) from fresh human normal lung and tumor tissues. The sequencing was analyzed by Pyro-Mark software, which automatically calculated each sequence percentage as a quantitative value and genotype. These pyro-sequencing results are representative data for 9 cultured cell lines and 10 sets of normal and tumor tissue specimens.

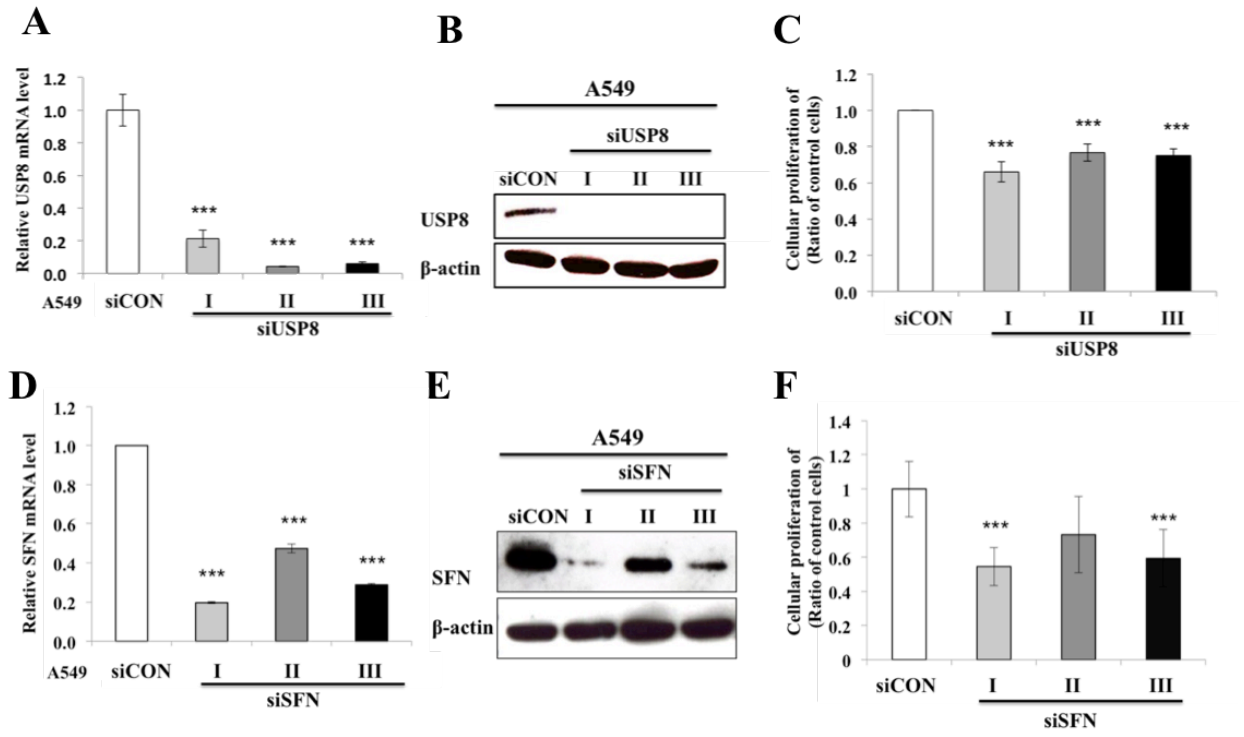

Fig. 10. Knockdown efficiency of siRNA-USP8 or -SFN in mRNA and protein levels and cellular proliferation.

A549 was transfected with three kinds of siRNA-USP8 (A-C), siRNA-SFN (D-F) or scrambled siRNA. Knockdown efficiency was confirmed at the mRNA and protein levels. (A and D) Total RNA was extracted from the cells after siRNA transfection for 24 h. USP8 or SFN mRNA were examined by real-time RT-PCR, and 18S was used as an internal control. (B and E) Total protein was extracted from the cells after siRNA transfection for 48 h. USP8 or SFN protein were analyzed by Western blot analysis. β-Actin was used as a control to verify equal loading of protein (20 μg). (C and F) Cellular proliferation was examined using WST-1 assay after siRNA transfection for 48 h. Among three siRNA sequences, the most effective siRNA-USP8-I and siRNA-SFN-I, were selected for further analysis.

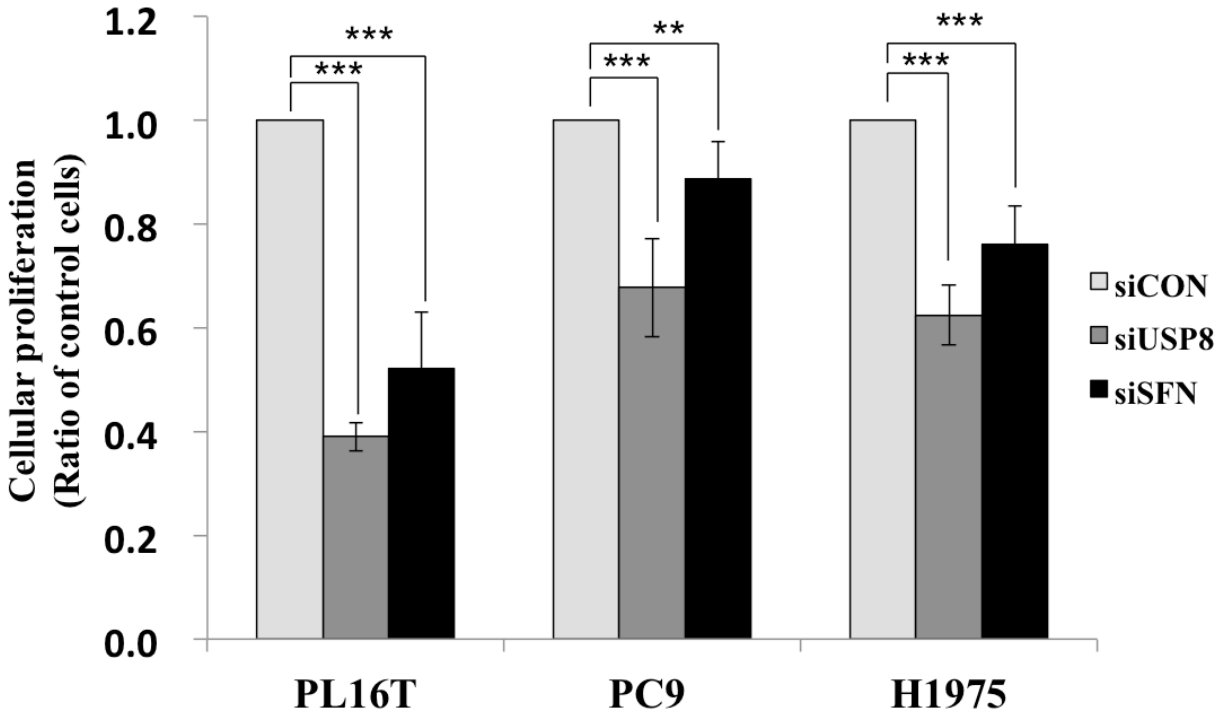

Fig. 11. Knockdown of USP8 or SFN regulates proliferation of lung adenocarcinoma cell lines.

Cellular proliferation was tested by WST-1 using PL16T (immortalized AIS cells) and the adenocarcinoma cell lines, PC9 and H1975, after siUSP8-I or siSFN transfection for 48 h.

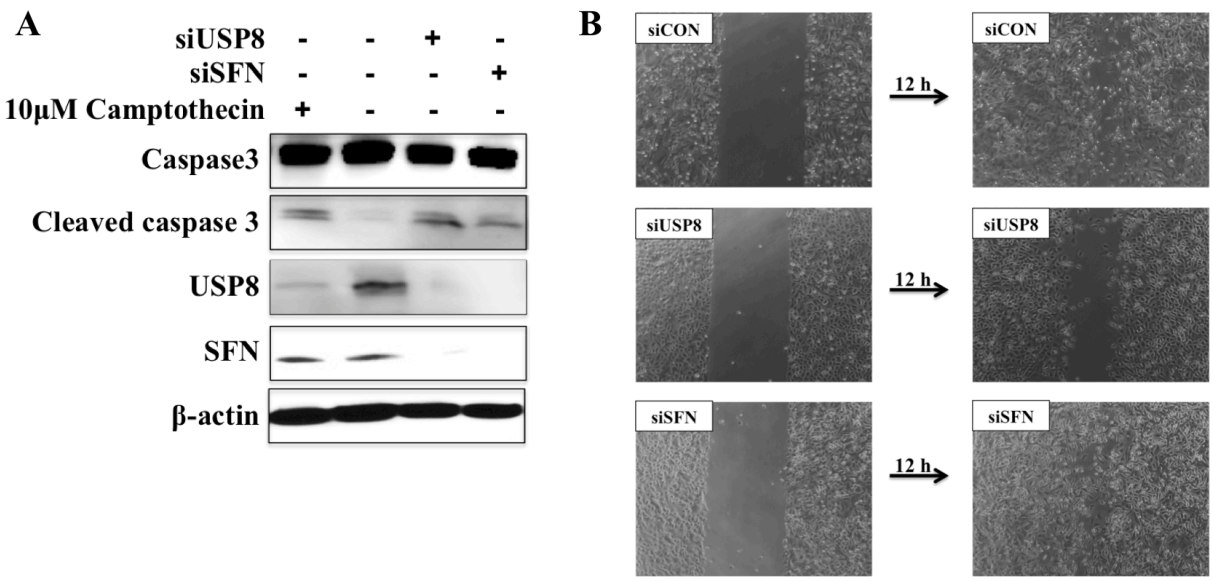

Fig. 12. Knockdown of USP8 or SFN regulates apoptosis and migration of PL16T.

(A) Expression of caspase 3 and cleaved caspase 3 as representative apoptosis-related proteins was analyzed using protein extracted for 48 h after siRNA transfection into PL16T. The positive control was pretreated with 10 μM camptothecin for 24 h at 37°C in a 5% CO_2 incubator before protein extraction. (B) *In vitro* migration activity was examined 12 h after scratch onto confluent cells. Knockdown of USP8 decreased wound healing activity compared to siCON or siSFN. PL16T, immortalized AIS cells.

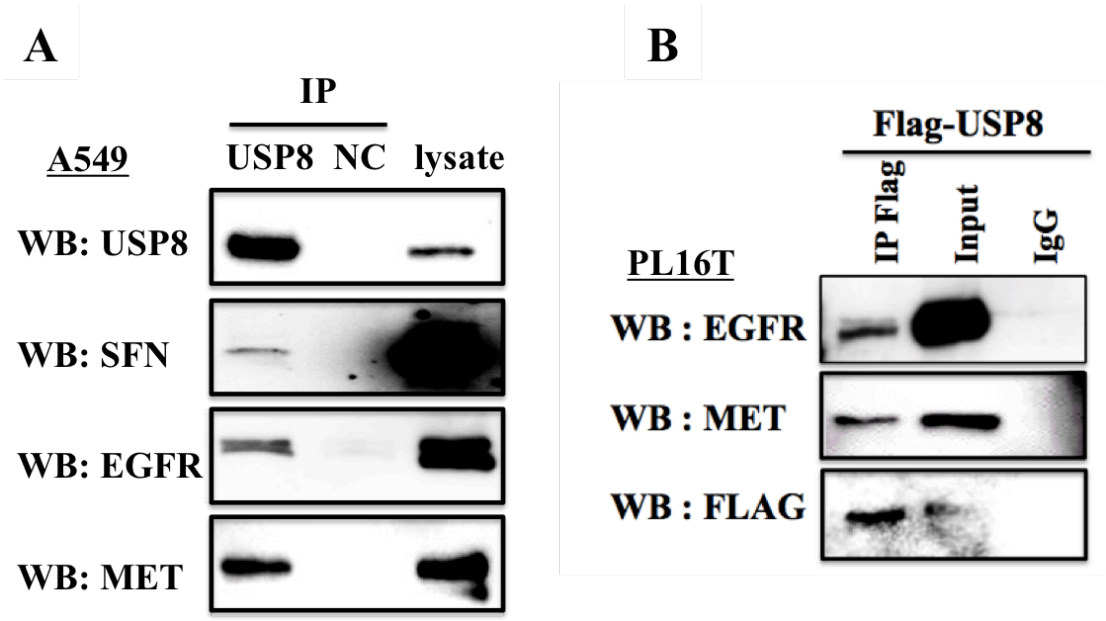

Fig. 13. USP8 binds with SFN and RTKs in lung adenocarcinoma cell lines.

(A) Endogenous interaction between USP8 and SFN or RTKs such as EGFR and MET was examined by Co-IP in A549 cells. As a negative control (NC), the cell lysate and protein A magnetic beads were incubated without antibody for 1 h at 4°C. (B) Co-IP using Flag antibody was performed after overexpression of Flag-USP8 in PL16T cells. As a negative control, the cell lysate and protein A with IgG antibody were incubated for 1 h at 4°C. The eluted IP sample was subjected to Western blot analysis using the indicated antibodies. PL16T, immortalized AIS cells.

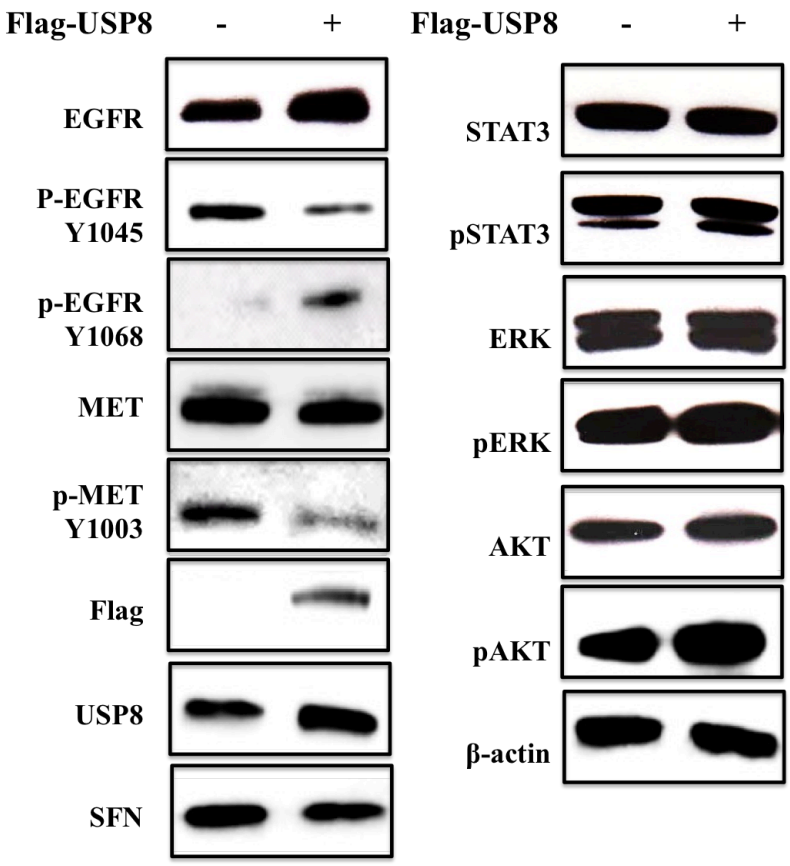

Fig. 14. Overexpression of USP8 enhances stabilization of RTKs in PL16T.

Flag-USP8 wild type was transfected into PL16T and expression of RTKs and downstream factors was analyzed by Western blot analysis. EGFR has mainly two phosphorylation sites, Y1045 for degradative pathway and Y1068 for proliferation-mediated pathway. MET Y1003 is a phosphorylation site for degradative pathway. β-Actin was used as a control to verify equal loading of protein (20 μg). PL16T, immortalized AIS cells.

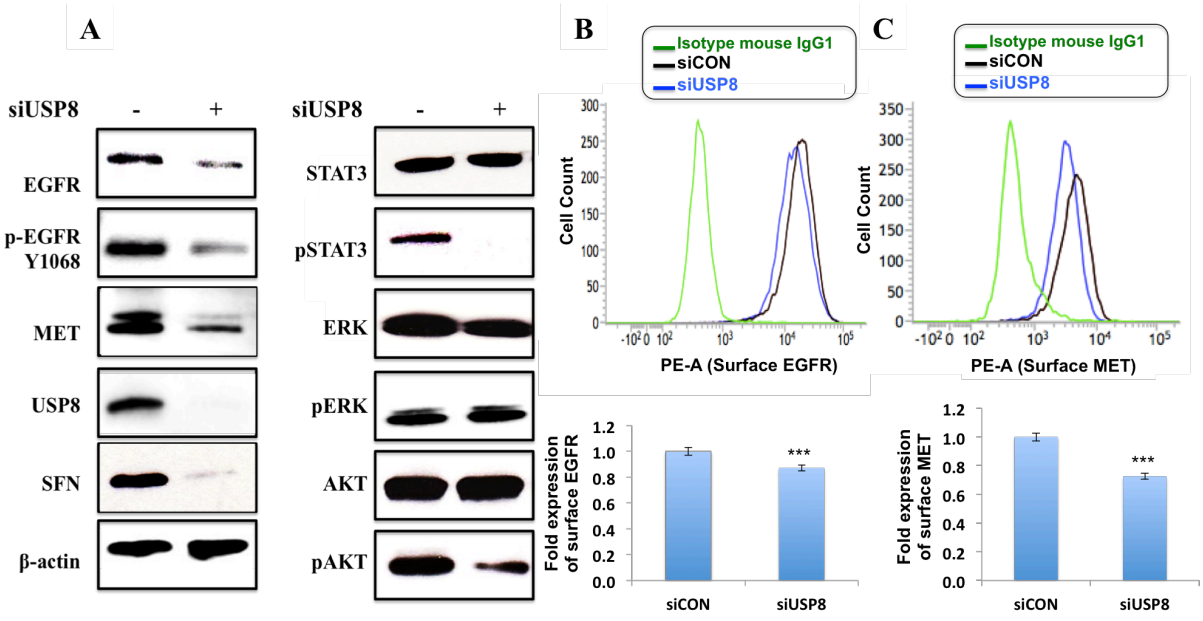

Fig. 15. Knockdown of USP8 downregulates SFN, surface RTKs, and the downstream factors in PL16T.

(A) Transfection efficiency of siUSP8 was evaluated by USP8 expression. Expression of SFN, RTKs, and the downstream factors were analyzed by Western blot analysis. β-Actin was used as a control to verify equal loading of protein (20 μg). EGFR (B) and MET (C) expression at the cell surface was verified by flow cytometry after transfection with siUSP8 under serum starvation. The column chart was drawn using the mean value of PE-A (n=3, t-test ***p<0.001). PL16T, immortalized AIS cells.

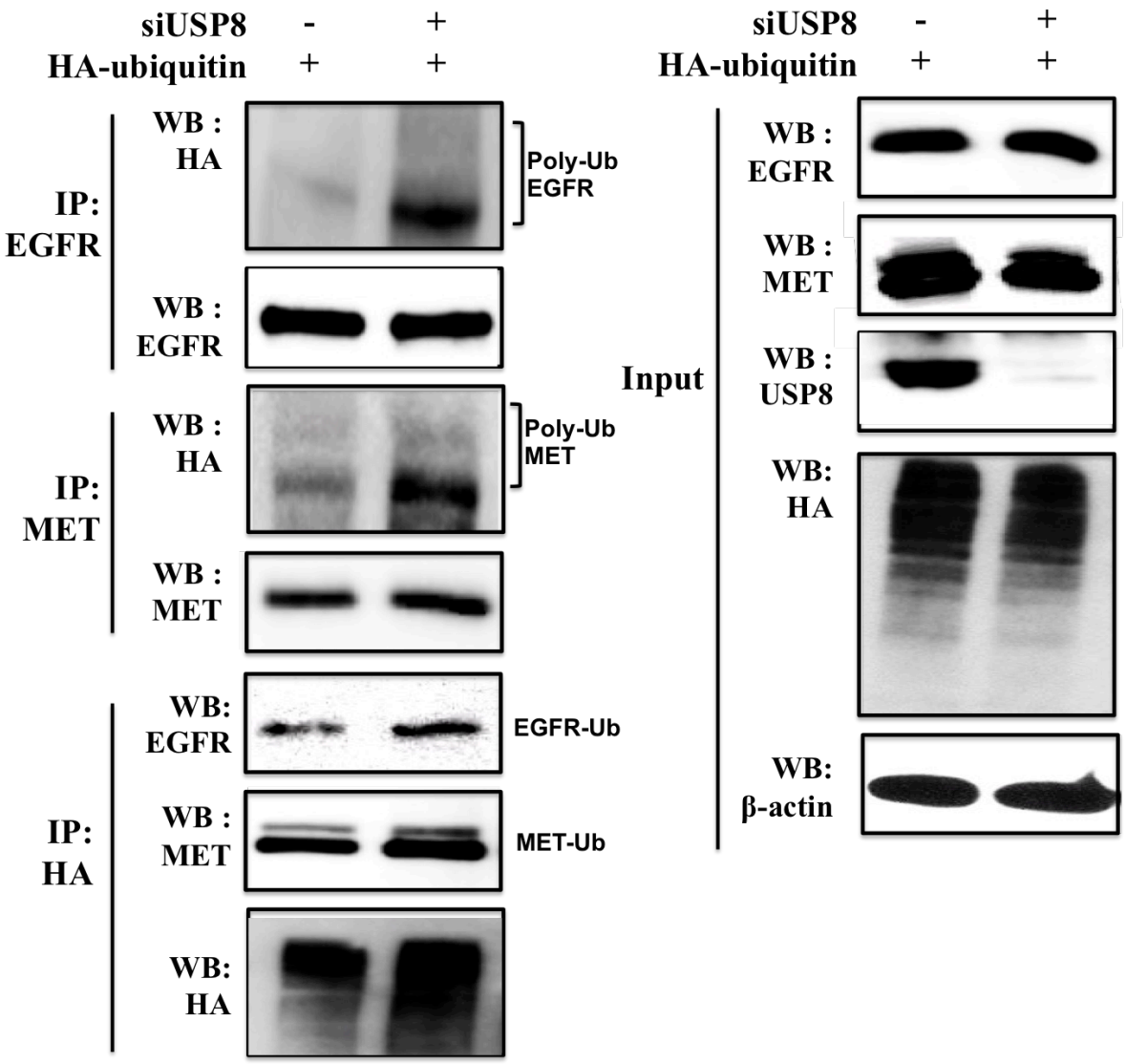

Fig. 16. Knockdown of USP8 increases ubiquitinated RTKs in PL16T.

Expression of ubiquitinated EGFR and MET was assessed by immunoprecipitation after transfection with siUSP8 accompanying the overexpression of HA-ubiquitin. The cells were treated with 25mM NH_4Cl (a lysosomal inhibitor) for 4 h, leading to accumulation of ubiquitinated EGFR or MET at the lysosome. PL16T, immortalized AIS cells.

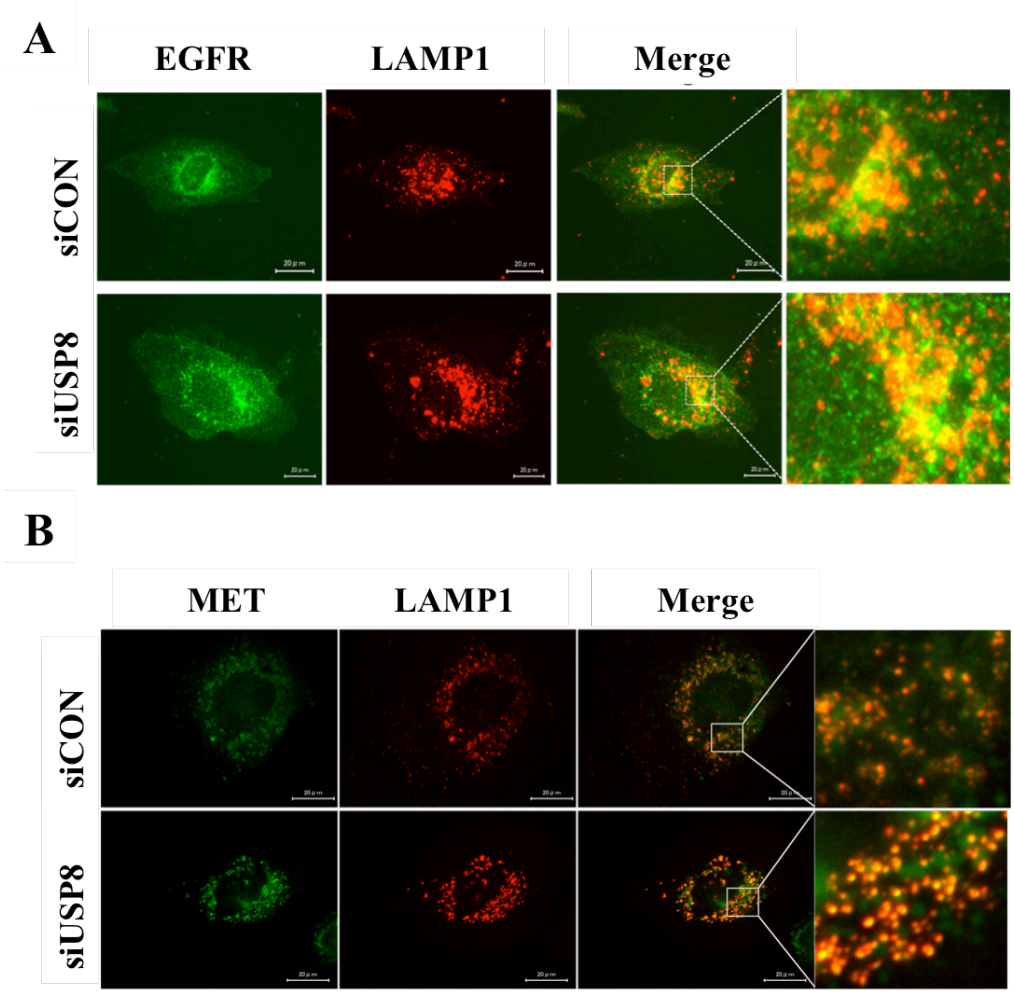

Fig. 17. Knockdown of USP8 induced accumulation of RTKs at lysosome in PL16T.

After siUSP8 transfection, ubiquitinated EGFR and MET, which were destined for lysosomal degradation, were assessed by IF employing LAMP1 (lysosomal marker) staining. EGFR (A) and MET (B) were immunostained with EGFR and MET antibody and accumulated at lysosome by treatment with 25mM NH_4Cl (lysosomal inhibitor) for 4 h. PL16T, immortalized AIS cells.

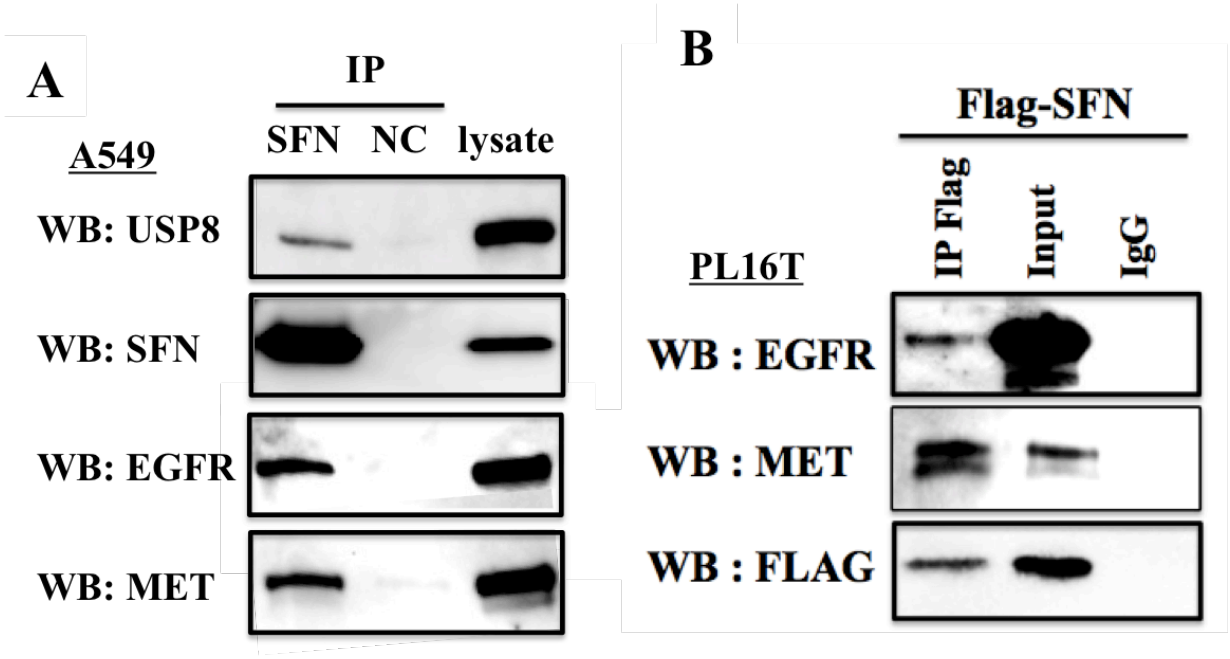

Fig. 18. SFN binds with USP8 and RTKs in lung adenocarcinoma cell lines.

(A) Endogenous interaction between USP8 and SFN or RTKs such as EGFR and MET was examined by Co-IP in A549 cells. As a negative control (NC), the cell lysate and protein A magnetic beads were incubated without antibody for 1 h at 4°C. (B) Co-IP using Flag antibody was performed after overexpression of Flag-SFN in PL16T. As a negative control, the cell lysate and protein A with IgG antibody were incubated for 1 h at 4°C. The eluted IP sample was subjected to Western blot analysis using the indicated antibodies. PL16T, immortalized AIS cells.

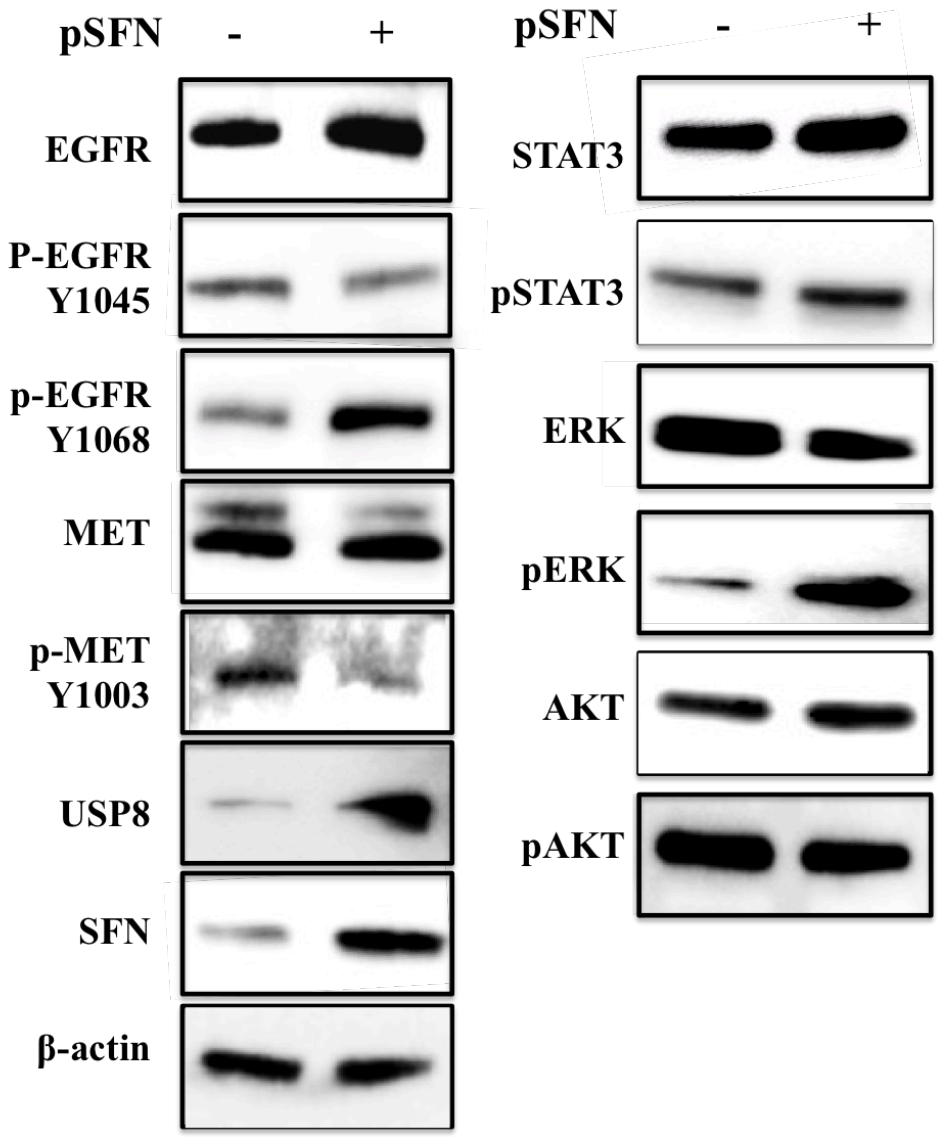

Fig. 19. Overexpression of SFN enhances stabilization of RTKs in PL16T.

After transfection with wild type SFN plasmid without any tag, expression of RTKs and downstream factors was analyzed by Western blot analysis. EGFR has mainly two phosphorylation sites, Y1045 for degradation pathway and Y1068 for proliferation-mediated pathway. MET Y1003 is a phosphorylation site for degradation pathway. β-Actin was used as a control to verify equal loading of protein (20 μg). PL16T, immortalized AIS cells.

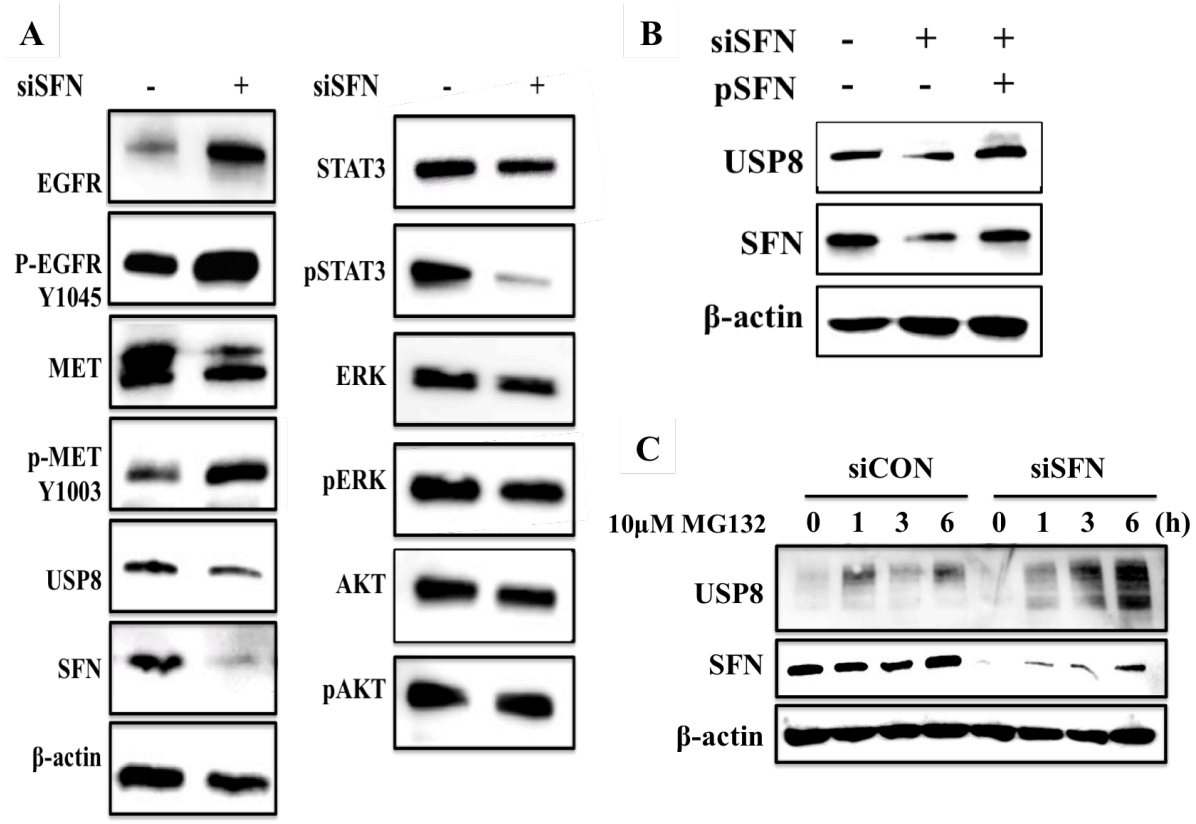

Fig. 20. Knockdown of SFN regulates USP8, RTKs, and the downstream factors in PL16T.

(A) Transfection efficiency of siSFN was evaluated by SFN expression. Expression of USP8, RTKs, and the downstream factors were analyzed by Western blot analysis using cells transfected with siSFN. β-Actin was used as a control to verify equal loading of protein (20 μg). (B) USP8 rescue assay was performed by Western blot analysis under co-transfection with siSFN for 24 h and subsequent overexpression of pSFN for 24 h. (C) After siSFN transfection for 48 h in A549, the cells treated 10 μM MG132 to inhibit USP8 proteasomal degradation in time course. The poly-ubiquitinated USP8 was detected by Western blot analysis. PL16T, immortalized AIS cells.

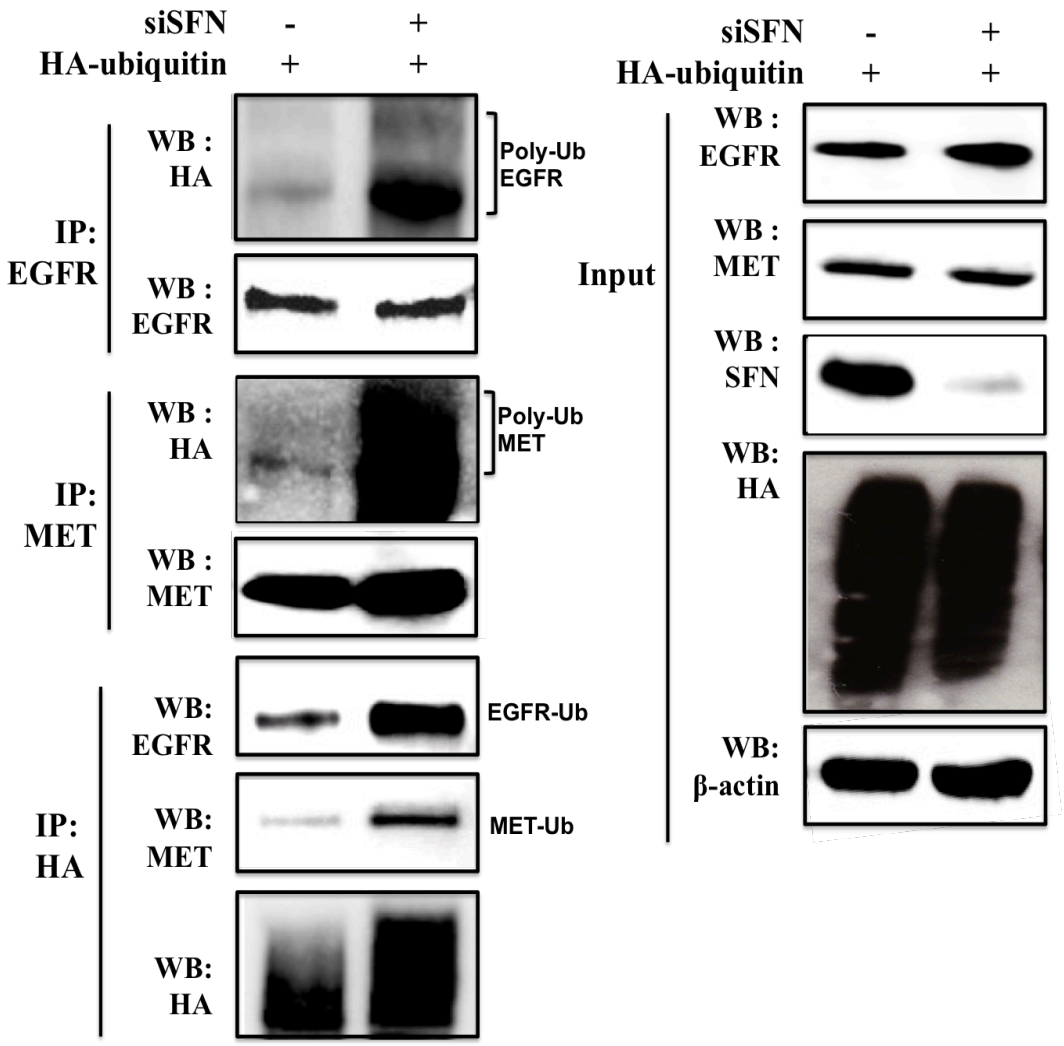

Fig. 21. Knockdown of SFN increases ubiquitinated RTKs in PL16T.

Expression of ubiquitinated EGFR and MET was assessed by immunoprecipitation after transfection with siSFN accompanying the overexpression of HA-ubiquitin. The cells were treated with 25mM NH_4Cl (a lysosomal inhibitor) for 4 h, leading to accumulation of ubiquitinated EGFR or MET at the lysosome. PL16T, immortalized AIS cells.

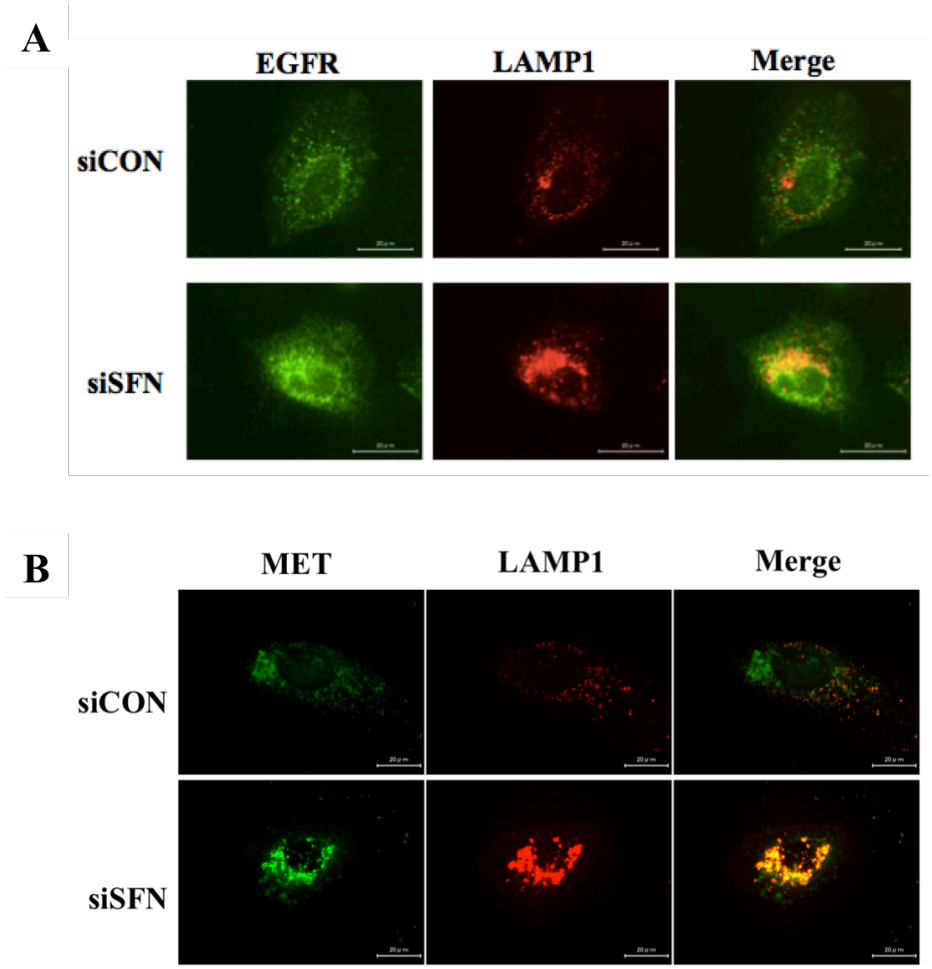

Fig. 22. Knockdown of SFN induces accumulation of RTKs at lysosome in PL16T.

After siSFN transfection, ubiquitinated EGFR and MET, which were destined for lysosomal degradation, were assessed by immunofluorescence staining employing LAMP1 (lysosomal marker) staining. EGFR and MET were immunostained with EGFR and MET antibody and accumulated at lysosome by treatment with 25mM NH_4Cl (lysosomal inhibitor) for 4 h. PL16T, immortalized AIS cells.

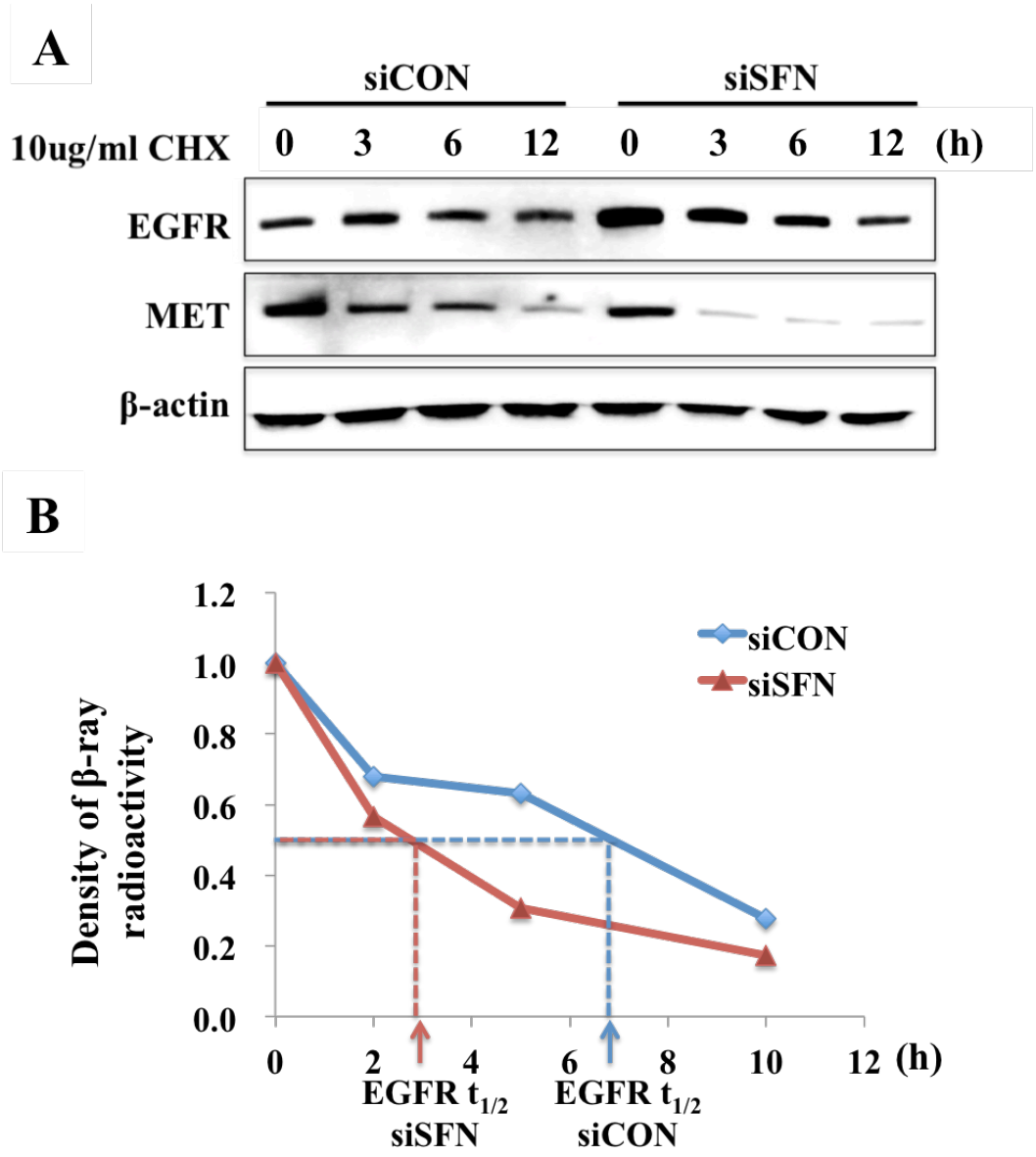

Fig. 23. Knockdown of SFN reduces half-life of RTKs in PL16T.

(A) The half-life of EGFR and MET was assessed by Western blot analysis after transfection with siSFN. The cells were treated with 10 μg/ml cycloheximide (CHX; a protein synthesis inhibitor) to block protein biosynthesis. (B) Pulse-chasing assay was performed to determine EGFR half-life after knockdown of SFN. The cells were labeled with ^{35}S-Met/Cys (10 μCi/ml) for 30 min and chased in time course 0, 2, 5, and 10 h. The metabolic labeled EGFR was scanned β–ray using Typhoon FLA7000 image analyzing system. PL16T, immortalized AIS cells.

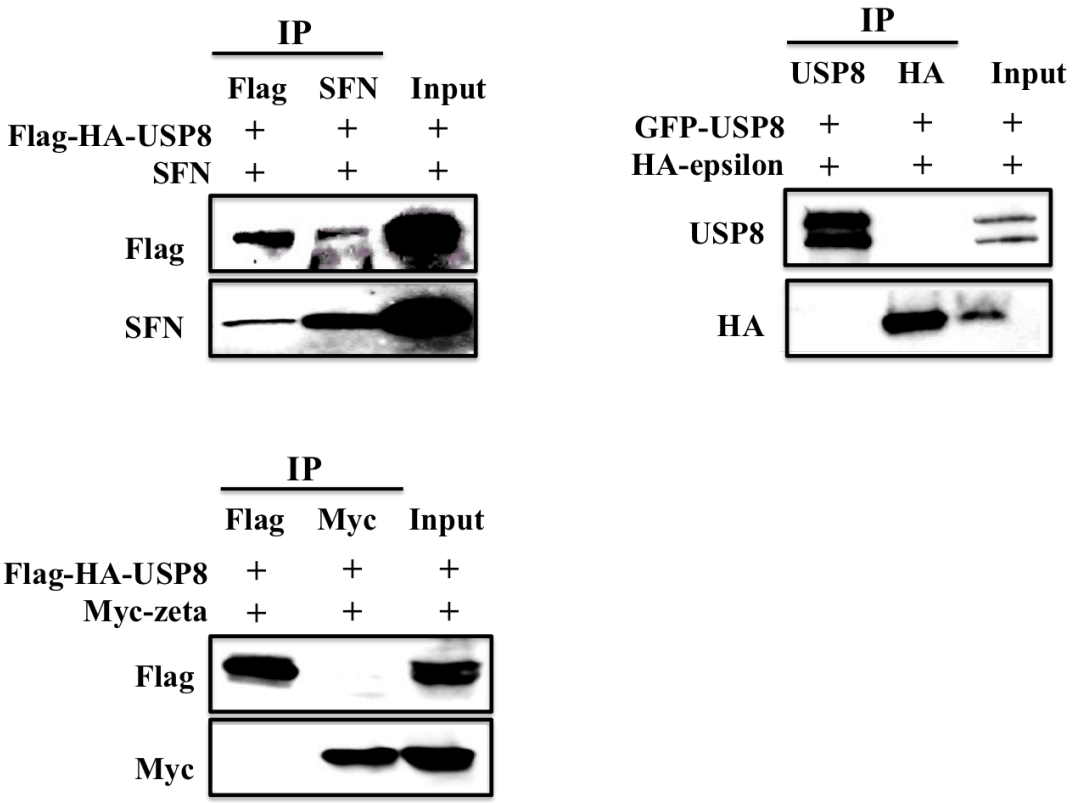

Fig. 24. USP8 specifically interacts with SFN among 14-3-3 proteins.

PL16T cells were transfected with various plasmids for 24 h to investigate the interaction between USP8 and 14-3-3 proteins (HA-epsilon: 14-3-3 epsilon, and Myc-zeta: 14-3-3 zeta). Co-IP was performed using the indicated antibodies. Only SFN showed binding with USP8. PL16T, immortalized AIS cells.

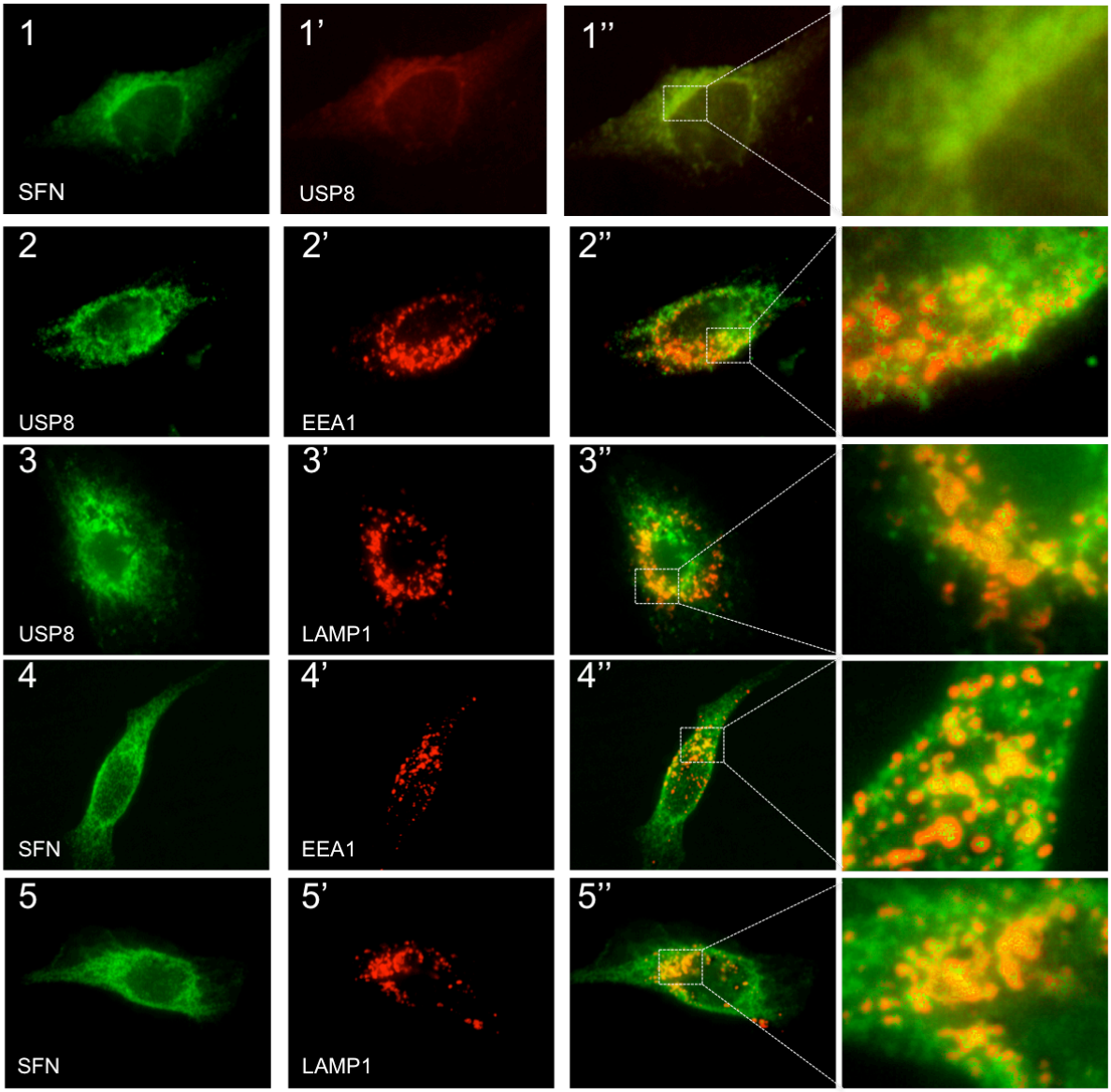

Fig. 25. USP8 and SFN co-localize in endosomes.

Localization of endogenous USP8 and SFN was examined by immunofluorescence staining. EEA1 and LAMP1 were used as early and late endosome markers, respectively. USP8 and SFN showed co-localization at the early and late endosome.

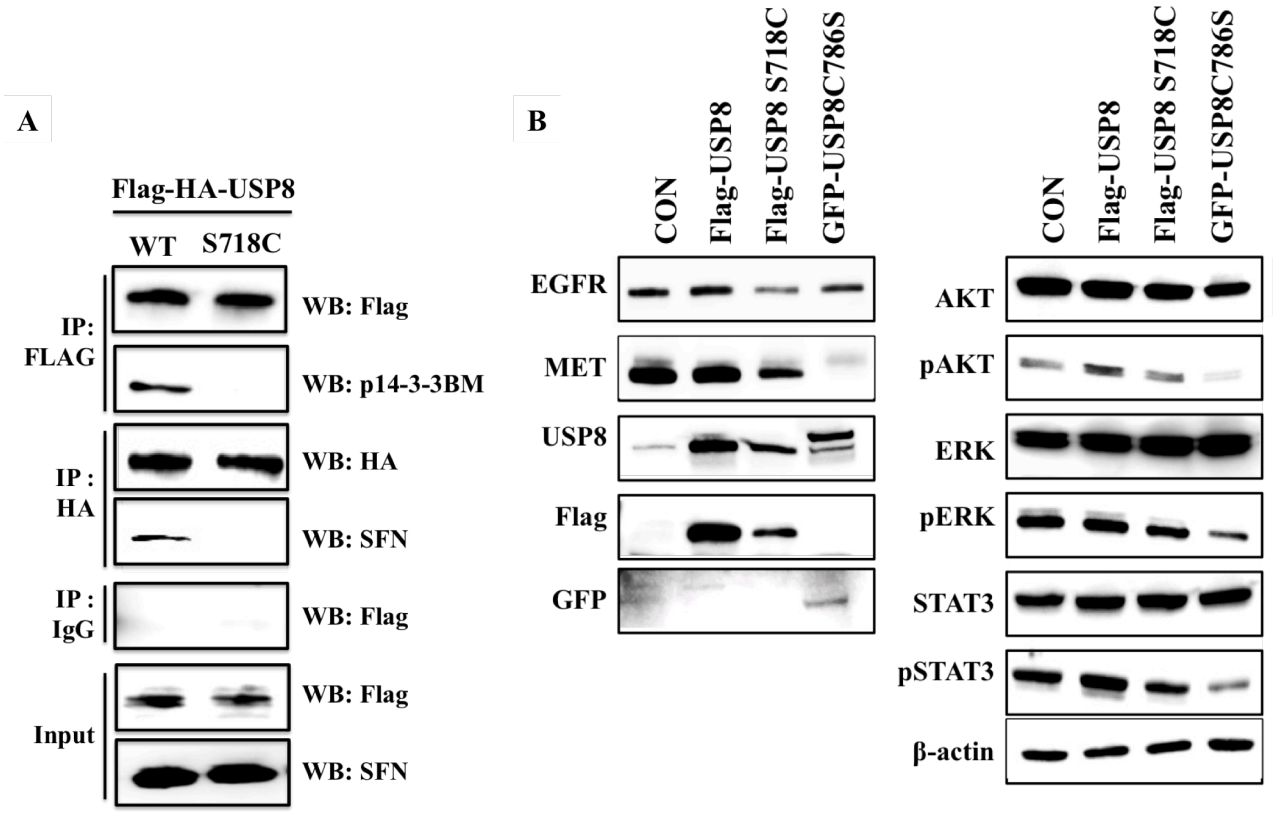

Fig. 26. Mutant USP8 impairs binding with SFN and decreases RTKs and their downstream factors.

(A) Mutant USP8 S718C contained a point mutation changing serine to cysteine at amino acid 718, which is one of the important phosphorylation residues of the 14-3-3 binding motif (AA715-720, RSYSSP) in USP8. Cells transfected with USP8 WT (wild type) or USP8 S718C (mutant) were tested for their interaction with SFN by co-IP. p14-3-3 BM (phospho-14-3-3 binding motif) indicates the active form of USP8 (phospho-USP8). (B) After transfection with the wild type or two kinds of mutant USP8, expression of RTKs and downstream factors was analyzed by Western blot analysis. GFP-USP8 C786S was used as a positive control to inhibit the deubiquitination activity of USP8. β-Actin was used as a control to verify equal loading of protein (20 μg).

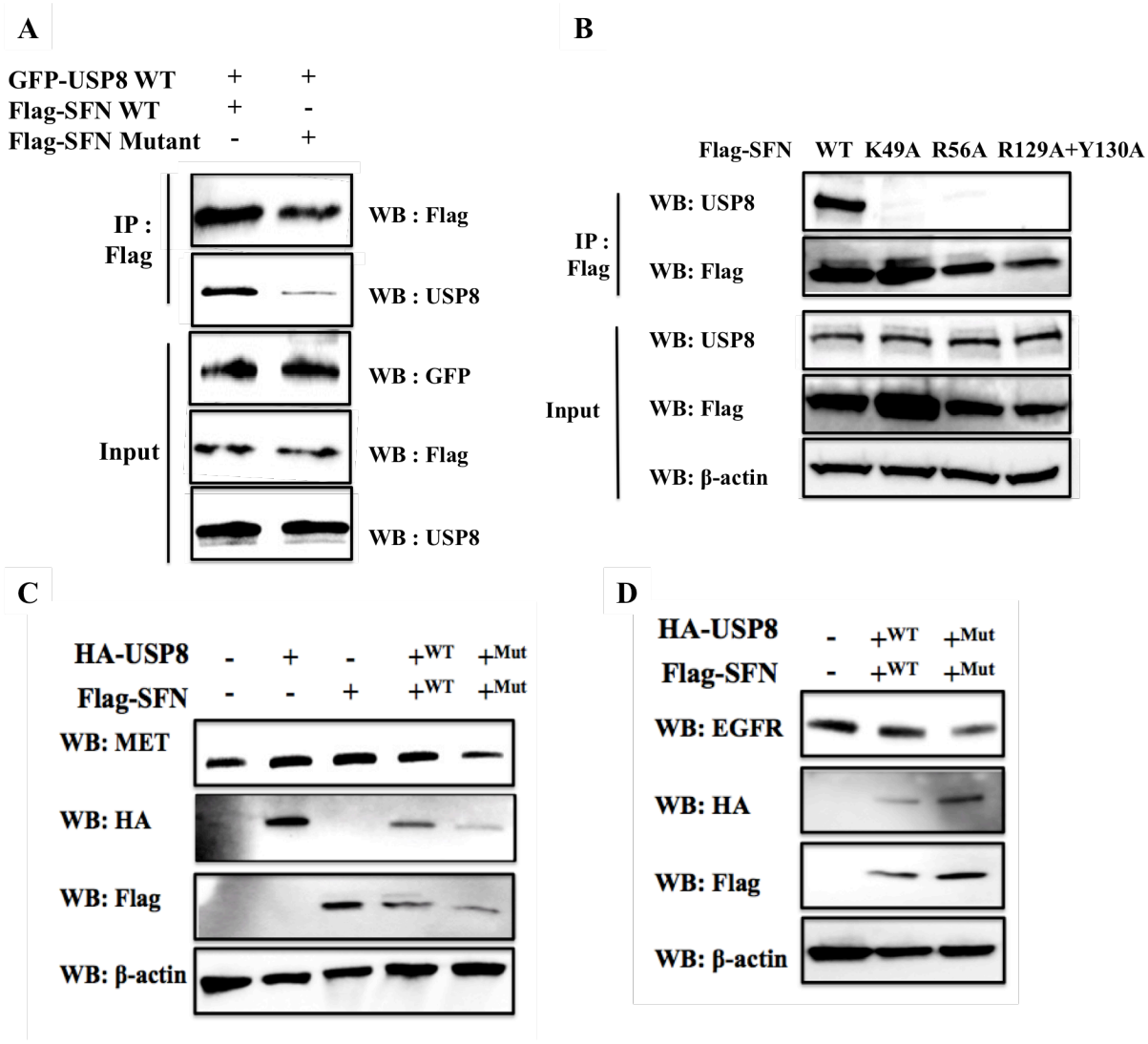

Fig. 27. Mutant SFN impairs binding with USP8 and decreases RTKs expression.

(A) Mutant SFN contained four multiple point mutations at 49, 56, 129, and 130 residues, which is the important residues for recognizing of phospho-target proteins such as RSYSSP for USP8. Cells transfected with SFN WT (wild type) or mutant SFN accompanying with USP8 WT were tested for their interaction with Flag by co-IP in PL16T. (B) Single point mutant SFN containing a single point mutation at 49, 56, 129 and 130 residues, respectively. Cells transfected with each single point mutant SFN was performed co-IP. (C, D) After transfection with the wild type or mutant USP8 and SFN, expression of RTKs and downstream factors was analyzed by Western blot analysis. β-Actin was used as a control to verify equal loading of protein (20 μg). PL16T, immortalized AIS cells.

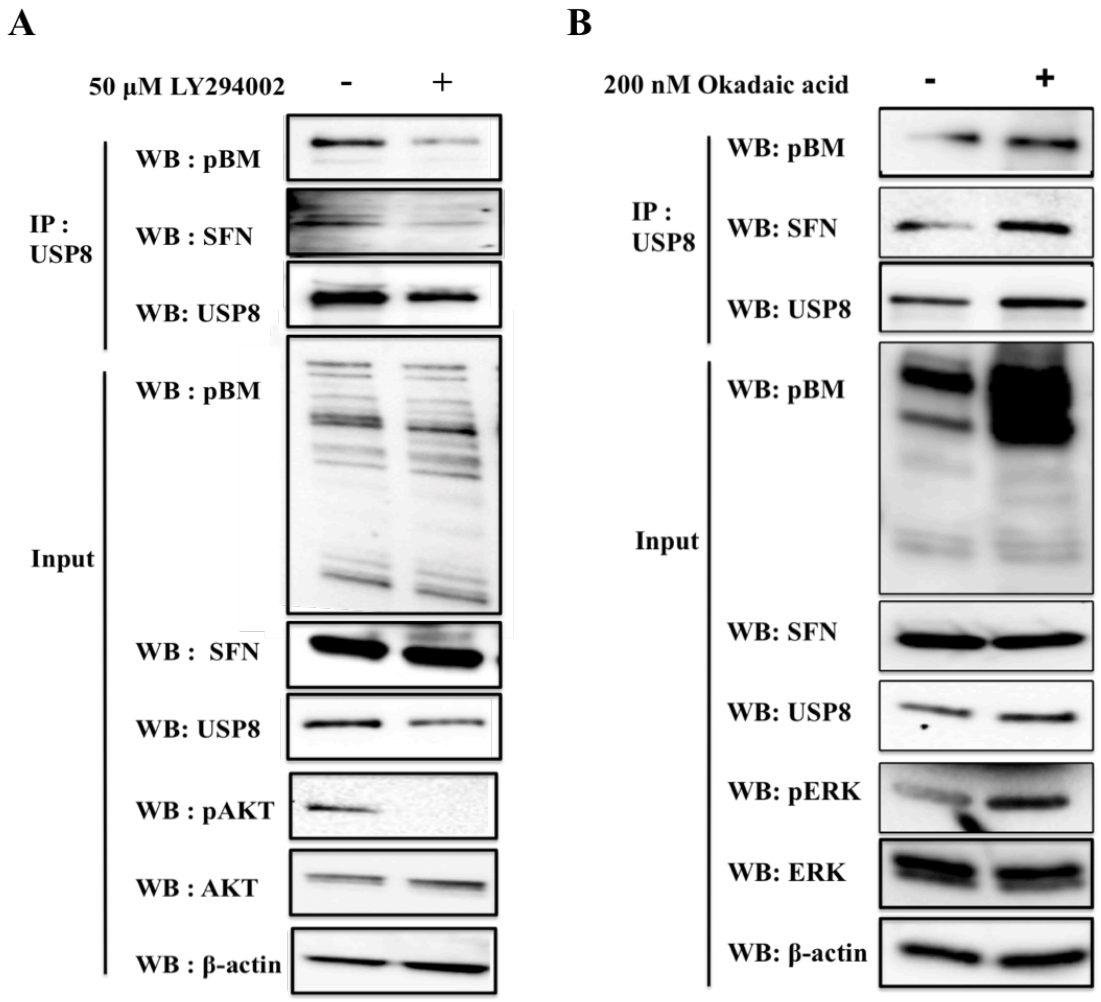

Fig. 28. SFN-USP8 complex is regulated by Serine/Threonine kinase and phosphatase.

SFN-USP8 complex was evaluated by co-IP and Western blot analysis. pBM is phospho 14-3-3 binding motif , indicating phospho-USP8 and that provides USP8 binding with SFN. (A) A549 cells were treated with 50 μM LY294002, an AKT (Serine/Threonine kinase) inhibitor for 1 h. pAKT was used as a positive control for Serine/Threonine kinase inhibitor. (B) A549 cells were treated with 200 nM okadaic acid, an PP1 or PP2A (Seine/Threonine phosphatase) specific inhibitor for 1 h. pERK was used as a positive control for Serine/Threonine phosphatase inhibitor. β-Actin was used as a control to verify equal loading of protein (20 μg).

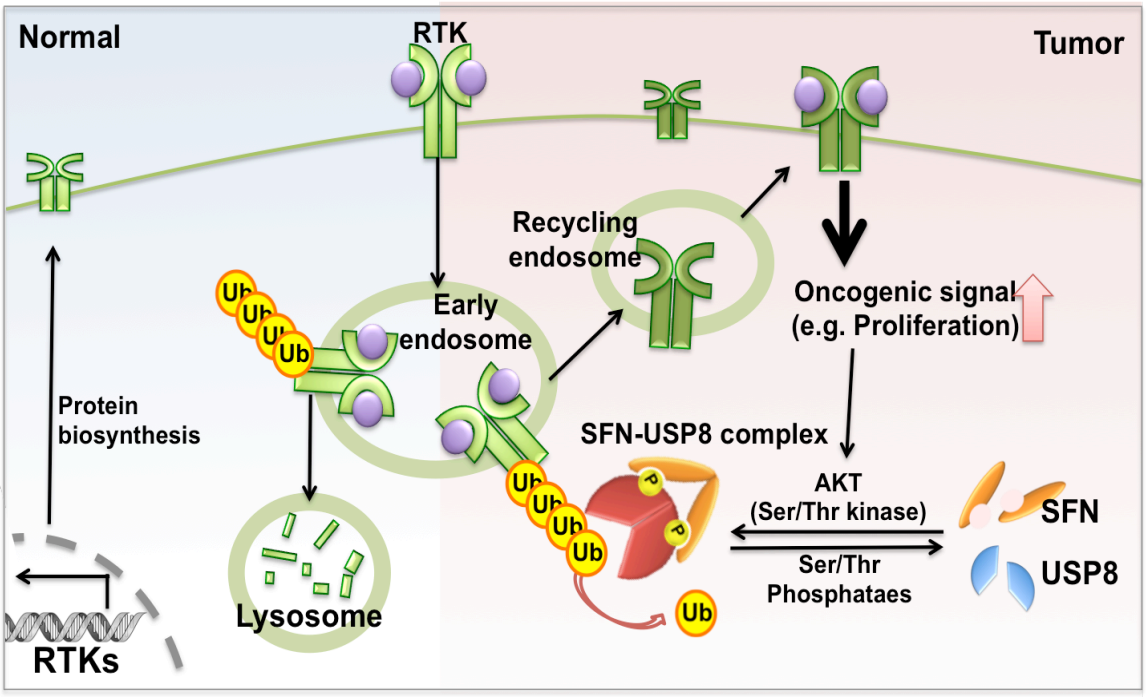

Fig. 29. A model for regulation pathway of RTKs in normal and tumor of lung cells.

Ligand-bound RTKs are internalized through endocytosis and form early endosomes. Some internalized RTKs are subjected to lysosomal degradation, but others undergo recycling back to the plasma membrane via recycling endosomes through USP8 activation. In normal cells, ubiquitinated RTKs maintain the balance between the recycling and degradation pathways, as well as physiologic regulation of biosynthesis. However, in tumor cells, SFN and USP8 show abnormal overexpression and their complex facilitates recycling of RTKs to the plasma membrane through deubiquitination of ubiquitinated RTKs. Subsequently, increased stabilization of RTKs on the plasma membrane contributes to aberrant cellular proliferation.

7. References

1. Siegel RL, Miller KD, Jemal A. Cancer statistics, 2016. CA: a cancer journal for clinicians. 2016;66(1):7-30.

2. Noguchi M, Morikawa A, Kawasaki M, Matsuno Y, Yamada T, Hirohashi S, et al. Small adenocarcinoma of the lung. Histologic characteristics and prognosis. Cancer. 1995;75(12):2844-52.

3. Noguchi M. Stepwise progression of pulmonary adenocarcinoma--clinical and molecular implications. Cancer metastasis reviews. 2010;29(1):15-21.

4. Saito M, Shiraishi K, Kunitoh H, Takenoshita S, Yokota J, Kohno T. Gene aberrations for precision medicine against lung adenocarcinoma. Cancer science. 2016;107(6):713-20.

5. Wilker EW, Grant RA, Artim SC, Yaffe MB. A structural basis for 14-3-3sigma functional specificity. The Journal of biological chemistry. 2005;280(19):18891-8.

6. Aghazadeh Y, Papadopoulos V. The role of the 14-3-3 protein family in health, disease, and drug development. Drug discovery today. 2016;21(2):278-87.

7. Yaffe MB, Rittinger K, Volinia S, Caron PR, Aitken A, Leffers H, et al. The structural basis for 14-3-3:phosphopeptide binding specificity. Cell. 1997;91(7):961-71.

8. Hermeking H. The 14-3-3 cancer connection. Nature reviews Cancer. 2003;3(12):931-43.

9. Smith AJ, Daut J, Schwappach B. Membrane proteins as 14-3-3 clients in functional regulation and intracellular transport. Physiology (Bethesda, Md). 2011;26(3):181-91.

10. Li Z, Liu JY, Zhang JT. 14-3-3sigma, the double-edged sword of human cancers. American journal of translational research. 2009;1(4):326-40.

11. Shiba-Ishii A, Noguchi M. Aberrant stratifin overexpression is regulated by tumor-associated CpG demethylation in lung adenocarcinoma. The American journal of pathology. 2012;180(4):1653-62.

12. Fraile JM, Quesada V, Rodriguez D, Freije JM, Lopez-Otin C. Deubiquitinases in cancer: new functions and therapeutic options. Oncogene. 2012;31(19):2373-88.

13. Alwan HA, van Leeuwen JE. UBPY-mediated epidermal growth factor receptor (EGFR) de-ubiquitination promotes EGFR degradation. The Journal of biological chemistry. 2007;282(3):1658-69.

14. Xia R, Jia H, Fan J, Liu Y, Jia J. USP8 promotes smoothened signaling by preventing its ubiquitination and changing its subcellular localization. PLoS biology. 2012;10(1):e1001238.

15. Mukai A, Yamamoto-Hino M, Awano W, Watanabe W, Komada M, Goto S. Balanced ubiquitylation and deubiquitylation of Frizzled regulate cellular responsiveness to Wg/Wnt. The EMBO journal. 2010;29(13):2114-25.

16. Wu X, Yen L, Irwin L, Sweeney C, Carraway KL, 3rd. Stabilization of the E3 ubiquitin ligase Nrdp1 by the deubiquitinating enzyme USP8. Molecular and cellular biology. 2004;24(17):7748-57.

17. Mizuno E, Iura T, Mukai A, Yoshimori T, Kitamura N, Komada M. Regulation of epidermal growth factor receptor down-regulation by UBPY-mediated deubiquitination at endosomes. Molecular biology of the cell. 2005;16(11):5163-74.

18. Meijer IM, van Leeuwen JE. ERBB2 is a target for USP8-mediated deubiquitination. Cellular signalling. 2011;23(2):458-67.

19. Smith GA, Fearnley GW, Abdul-Zani I, Wheatcroft SB, Tomlinson DC, Harrison MA, et al. VEGFR2 Trafficking, Signaling and Proteolysis is Regulated by the Ubiquitin Isopeptidase USP8. Traffic (Copenhagen, Denmark). 2016;17(1):53-65.

20. Takeuchi K, Ito F. Receptor tyrosine kinases and targeted cancer therapeutics. Biological & pharmaceutical bulletin. 2011;34(12):1774-80.

21. Byun S, Lee SY, Lee J, Jeong CH, Farrand L, Lim S, et al. USP8 is a novel target for overcoming gefitinib resistance in lung cancer. Clinical cancer research : an official journal of the American Association for Cancer Research. 2013;19(14):3894-904.

22. Naviglio S, Mattecucci C, Matoskova B, Nagase T, Nomura N, Di Fiore PP, et al. UBPY: a growth-regulated human ubiquitin isopeptidase. The EMBO journal. 1998;17(12):3241-50.

23. Niendorf S, Oksche A, Kisser A, Lohler J, Prinz M, Schorle H, et al. Essential role of ubiquitin-specific protease 8 for receptor tyrosine kinase stability and endocytic trafficking in vivo. Molecular and cellular biology. 2007;27(13):5029-39.

24. Greig MJ, Niessen S, Weinrich SL, Feng JL, Shi M, Johnson TO. Effects of Activating Mutations on EGFR Cellular Protein Turnover and Amino Acid Recycling Determined Using SILAC Mass Spectrometry. International journal of cell biology. 2015;2015:798936.

25. Tsiambas E, Lefas AY, Georgiannos SN, Ragos V, Fotiades PP, Grapsa D, et al. EGFR gene deregulation mechanisms in lung adenocarcinoma: A molecular review. Pathology, research and practice. 2016;212(8):672-7.

26. Bronte G, Rizzo S, La Paglia L, Adamo V, Siragusa S, Ficorella C, et al. Driver mutations and differential sensitivity to targeted therapies: a new approach to the treatment of lung adenocarcinoma. Cancer treatment reviews. 2010;36 Suppl 3:S21-9.

27. Juchum M, Gunther M, Laufer SA. Fighting cancer drug resistance: Opportunities and challenges for mutation-specific EGFR inhibitors. Drug resistance updates : reviews and commentaries in antimicrobial and anticancer chemotherapy. 2015;20:12-28.

28. Maroun CR, Rowlands T. The Met receptor tyrosine kinase: a key player in oncogenesis and drug resistance. Pharmacology & therapeutics. 2014;142(3):316-38.

29. Sui X, Kong N, Zhu M, Wang X, Lou F, Han W, et al. Cotargeting EGFR and autophagy signaling: A novel therapeutic strategy for non-small-cell lung cancer. Molecular and clinical oncology. 2014;2(1):8-12.

30. Nakayama KI, Nakayama K. Ubiquitin ligases: cell-cycle control and cancer. Nature reviews Cancer. 2006;6(5):369-81.

31. Hussain S, Zhang Y, Galardy PJ. DUBs and cancer: the role of deubiquitinating enzymes as oncogenes, non-oncogenes and tumor suppressors. Cell cycle (Georgetown, Tex). 2009;8(11):1688-97.

32. Mohapatra B, Ahmad G, Nadeau S, Zutshi N, An W, Scheffe S, et al. Protein tyrosine kinase regulation by ubiquitination: critical roles of Cbl-family ubiquitin ligases. Biochimica et biophysica acta. 2013;1833(1):122-39.

33. Mukhopadhyay D, Riezman H. Proteasome-independent functions of ubiquitin in endocytosis and signaling. Science (New York, NY). 2007;315(5809):201-5.

34. Travis WD, Brambilla E, Noguchi M, Nicholson AG, Geisinger KR, Yatabe Y, et al. International association for the study of lung cancer/american thoracic society/european respiratory society international multidisciplinary classification of lung adenocarcinoma. Journal of thoracic oncology : official publication of the International Association for the Study of Lung Cancer. 2011;6(2):244-85.

35. Travis WD, Brambilla E, Nicholson AG, Yatabe Y, Austin JH, Beasley MB, et al. The 2015 World Health Organization Classification of Lung Tumors: Impact of Genetic, Clinical and Radiologic Advances Since the 2004 Classification. Journal of thoracic oncology : official publication of the International Association for the Study of Lung Cancer. 2015;10(9):1243-60.

36. Shiba-Ishii A, Kano J, Morishita Y, Sato Y, Minami Y, Noguchi M. High expression of stratifin is a universal abnormality during the course of malignant progression of early-stage lung adenocarcinoma. International journal of cancer. 2011;129(10):2445-53.

37. Shimada A, Kano J, Ishiyama T, Okubo C, Iijima T, Morishita Y, et al. Establishment of an immortalized cell line from a precancerous lesion of lung adenocarcinoma, and genes highly expressed in the early stages of lung adenocarcinoma development. Cancer science. 2005;96(10):668-75.

38. Simon E, Kornitzer D. Pulse-chase analysis to measure protein degradation. Methods in enzymology. 2014;536:65-75.

39. Sbiera S, Deutschbein T, Weigand I, Reincke M, Fassnacht M, Allolio B. The New Molecular Landscape of Cushing's Disease. Trends in endocrinology and metabolism: TEM. 2015;26(10):573-83.

40. Huang WG, Cheng AL, Chen ZC, Peng F, Zhang PF, Li MY, et al. Targeted proteomic analysis of 14-3-3sigma in nasopharyngeal carcinoma. The international journal of biochemistry & cell biology. 2010;42(1):137-47.

41. Ballif BA, Cao Z, Schwartz D, Carraway KL, 3rd, Gygi SP. Identification of 14-3-3epsilon substrates from embryonic murine brain. Journal of proteome research. 2006;5(9):2372-9.

42. Dufner A, Kisser A, Niendorf S, Basters A, Reissig S, Schonle A, et al. The ubiquitin-specific protease USP8 is critical for the development and homeostasis of T cells. Nature immunology. 2015;16(9):950-60.

43. Panner A, Crane CA, Weng C, Feletti A, Fang S, Parsa AT, et al. Ubiquitin-specific protease 8 links the PTEN-Akt-AIP4 pathway to the control of FLIPS stability and TRAIL sensitivity in glioblastoma multiforme. Cancer research. 2010;70(12):5046-53.

44. Reincke M, Sbiera S, Hayakawa A, Theodoropoulou M, Osswald A, Beuschlein F, et al. Mutations in the deubiquitinase gene USP8 cause Cushing's disease. Nature genetics. 2015;47(1):31-8.

45. Ma ZY, Song ZJ, Chen JH, Wang YF, Li SQ, Zhou LF, et al. Recurrent gain-of-function USP8 mutations in Cushing's disease. Cell research. 2015;25(3):306-17.

46. Perez-Rivas LG, Theodoropoulou M, Ferrau F, Nusser C, Kawaguchi K, Stratakis CA, et al. The Gene of the Ubiquitin-Specific Protease 8 Is Frequently Mutated in Adenomas Causing Cushing's Disease. The Journal of clinical endocrinology and metabolism. 2015;100(7):E997-1004.

47. Shiba-Ishii A, Kim Y, Shiozawa T, Iyama S, Satomi K, Kano J, et al. Stratifin accelerates progression of lung adenocarcinoma at an early stage. Molecular cancer. 2015;14:142.

48. Meijer IM, Kerperien J, Sotoca AM, van Zoelen EJ, van Leeuwen JE. The Usp8 deubiquitination enzyme is post-translationally modified by tyrosine and serine phosphorylation. Cellular signalling. 2013;25(4):919-30.

49. Zhu G, Fan Z, Ding M, Zhang H, Mu L, Ding Y, et al. An EGFR/PI3K/AKT axis promotes accumulation of the Rac1-GEF Tiam1 that is critical in EGFR-driven tumorigenesis. Oncogene. 2015;34(49):5971-82.

50. Devarakonda S, Morgensztern D, Govindan R. Genomic alterations in lung adenocarcinoma. The Lancet Oncology. 2015;16(7):e342-51.

51. Bansal P, Osman D, Gan GN, Simon GR, Boumber Y. Recent Advances in Targetable Therapeutics in Metastatic Non-Squamous NSCLC. Frontiers in oncology. 2016;6:112.

52. Kaplan A, Bueno M, Fournier AE. Extracellular functions of 14-3-3 adaptor proteins. Cellular signalling. 2017;31:26-30.

53. Medina A, Ghaffari A, Kilani RT, Ghahary A. The role of stratifin in fibroblast-keratinocyte interaction. Molecular and cellular biochemistry. 2007;305(1-2):255-64.

54. McLean JB, Moylan JS, Horrell EM, Andrade FH. Proteomic analysis of media from lung cancer cells reveals role of 14-3-3 proteins in cachexia. Frontiers in physiology. 2015;6:136.

55. Milane L, Singh A, Mattheolabakis G, Suresh M, Amiji MM. Exosome mediated communication within the tumor microenvironment. Journal of controlled release : official journal of the Controlled Release Society. 2015;219:278-94.

56. Muller L, Hong CS, Stolz DB, Watkins SC, Whiteside TL. Isolation of biologically-active exosomes from human plasma. Journal of immunological methods. 2014;411:55-65.

57. Clague MJ, Barsukov I, Coulson JM, Liu H, Rigden DJ, Urbe S. Deubiquitylases from genes to organism. Physiological reviews. 2013;93(3):1289-315.

58. Scaltriti M, Baselga J. The epidermal growth factor receptor pathway: a model for targeted therapy. Clinical cancer research : an official journal of the American Association for Cancer Research. 2006;12(18):5268-72.

59. Organ SL, Tsao MS. An overview of the c-MET signaling pathway. Therapeutic advances in medical oncology. 2011;3(1 Suppl):S7-s19.

Acknowledgements

So do not fear, for I am with you; do not be dismayed, for I am your God. I will strengthen you and help you; I will uphold you with my righteous right hand.

-Isaiah 41:10-

First of all, I would like to thank the supreme power the almighty God who is obviously the one has always guided me to work on the one has always guided me to work on the right path of life. Without his grace this project could not become a reality.

My deep gratitude goes to advisor professor Masayuki Noguchi, who expertly guided me through my graduate education and who shared the excitement of four years of discovery. His unwavering enthusiasm for physics kept me constantly engaged with my research, and his personal generosity helped make my time enjoyable at Tsukuba.

My appreciation also extends to advisor assistant professor Aya Shiba. Her mentoring and encouragement have been especially valuable and her early insights launched the greater part of this dissertation and publication.

I am highly obliged in taking instructive comments and research supports to sincerely thanks to Prof. Mitsuyasu Kato, Prof. Hideo Ichimura, Dr. Atsushi Kawaguchi, Dr. Yuji Funakoshi, Dr. Hiroyuki Suzuki, and Dr. Masafumi Muratani.

I also thank to all of our laboratory members with warm heart and genuine kindness to help sustain a positive atmosphere in lab.

Moreover, I would like to thank my former advisor professor Hwajin Park, who gave me high motivation and opportunity to study in Japan from long time ago as like his academic life with joy and enthusiasm.

I also very thank to my bible teachers, pastor Chae and missionary Kim and all of my friends for praying to make the study a well-done achievement.

Above ground, I am indebted to my family, whose value to me only grows with age and family-in-law for love and encouragement at all the time.

Lastly, I would like to express my gratitude to my husband, Frank SangJoon, who is my champion from deep down in my heart and blesses me with love and prayer. I want to give special thanks to my daughter, Samantha SeolA and my son to-be-born, Joshua who are the greatest delight of my life.

Thank you.

YunJung Kim

University of Tsukuba

September 2017.